

A HYBRID FINITE ELEMENT ANALYSIS OF SHOT PEEN CONTOUR FORMING
USING RESIDUAL STRESS MEASUREMENTS

A Thesis by

James Michael Wagner, Jr.

Bachelor of Engineering, University of Pittsburgh, Pittsburgh, PA, USA, 2000

Submitted to the Department of Mechanical Engineering
and the faculty of the Graduate School of
Wichita State University
in partial fulfillment of
the requirements for the degree of
Master of Science

May 2013

© Copyright 2013 by James Michael Wagner, Jr.

All Rights Reserved

WARNING - This document contains technical data whose export is restricted by the Arms Export Control Act (Title 22, U.S. C., Sec 2751, et seq.) or the Export Administration Act of 1979, as amended, Title 50, U.S.C., App. 2401 et seq. Violations of these export laws are subject to severe criminal penalties. Disseminate in accordance with provisions of DoD Directive 5230.25. The information herein contains Export Controlled data under Export Control Classification Number EAR99, no license required.

A HYBRIC FINITE ELEMENT ANALYSIS OF SHOT PEEN CONTOUR FORMING
USING RESIDUAL STRESS MEASUREMENTS

The following faculty members have examined the final copy of this thesis for the form and content, and recommend that it be accepted in partial fulfillment of the requirement for the degree of Master of Science with a major in Mechanical Engineering.

Hamid Lankarani, Committee Chair

Ramazan Asmatulu, Committee Member

Krishna Krishnan, Committee Member

Rasoul Moradi, Committee Member

DEDICATION

To
my parents, my beautiful wife and my son Lysander.

ACKNOWLEDGEMENTS

I would like to thank Spirit AeroSystems, Inc. for allowing me to use the work I conducted over the last few years and the data contained in this document. The people that work at Spirit AeroSystems, Inc., especially Thanh Le and Darrell Wade, for their instruction over the years, and Elmer in Shot Peening, whose work helped me complete the project. I would also like to thank Dr. Lankarani for his continued guidance and support in completing my thesis. Special thanks to my other committee members Dr. Asmatulu, Dr. Krishnan and Dr. Moradi. Lastly, but not least, I must thank my entire family for all of their support.

ABSTRACT

In order to develop surfaces that have the proper curvature for aerospace structures, it is sometimes necessary to use shot peen forming, also known as contour forming, to create the desired shape in a piece of metal. Since the preferred metal in aerospace continues to be aluminum and its alloys, this study will concentrate on the effects of shot peening on aluminum.

Typically, shot intensity is measured using standard Almen strips made from cold rolled SAE 1070 spring steel. Since the effects of the shot on aluminum is the chief concern of this study, aluminum strips of the same size and thickness will be used to determine the intensity of the shot on aluminum parts. These strips will be exposed for different amounts of time to different intensities, measured using the steel Almen strips, and then the intensity (or arc height) will be measured on the aluminum strips. The residual stresses in these strips will then be measured using the hole drill method (ASTM E837).

The stresses from the residual stress test will then be used to develop a finite element model that simulates the aluminum strips and the deformation in them. The model will then be calibrated with the empirical data. From there, it will be the goal of this study to be able to predict the deformation of aluminum parts when exposed to certain shot peen intensities. This will enable more efficient contour forming processes with less rework. Furthermore, the trial and error of a manual process can be avoided with the use of robotics. Robotics/Automation can also help in creating more consistent results.

TABLE OF CONTENTS

Chapter		Page
1	INTRODUCTION	1
1.1	Background.....	1
1.2	Literature Review	2
1.3	Objective.....	5
2	METHODOLOGY	6
2.1	Specific Tasks.....	6
2.2	Analytical Calculations.....	7
2.2.1	Volume of an Indent	7
2.2.2	Energy and Work.....	7
2.2.3	Brinell Hardness Number	9
2.2.4	An Illustrative Example.....	10
2.3	Dynamic Modeling	11
2.4	Shot peening	17
2.5	Measuring Residual Stress.....	21
2.6	Quasi-Static Contact/Impact Modeling and Analysis.....	22
3	COMPARISON OF RESULTS AND DISCUSSION	26
3.1	Results from Hybrid FEA Simulations of Shot Peening	26
3.2	Comparison of Empirical Data and Hybrid FEA Simulations	42
4	CONCLUSIONS AND RECOMMENDATIONS	44
4.1	Conclusions.....	44
4.2	Recommendations for Future Studies.....	45
	REFERENCES	47

LIST OF FIGURES

Figure	Page
1 - A shot stream from a nozzle impacts a strip of metal (ceramics.org)	1
2 – The work done to the substrate is observed in the difference between the drop height and the height of the bounce of the shot.....	8
3 - Work done per unit volume is simplified by calculating the compression of a representative cylinder.	9
4 - Brinell Hardness Number	10
5 - Geometry of an indent	11
6 - Results of dynamic analysis using MSC Marc Mentat to model the shot and aluminum plate.	12
7 - Graph showing the expected stress distribution through the thickness of a shot peened surface. (Champaign, 2001)	13
8 - Symmetric model of single shot and a section of an aluminum plate. Modeled using MSC Marc Mentat.....	14
9 - Graph of the results of the FEA model. Components of the residual stress through the thickness of the part is compressive near the surface and the tensile residual stress deeper below the surface.	15
10 - Results showing the displacement of an aluminum almen strip with residual stresses measured using the hole drill method.	16
11 - Steel Almen strips on the left and Aluminum Almen Strips on the right, labeled with exposure time and arc heights measured in ten thousandths of an inch.	17
12 - Graph of the Arc Height of the 7075-T6 strips vs the exposure time/passes.	18
13 - Exposure Time/Passes vs. Arc height as measured manually by Elmer and using a Magnet to hold the strip in an Almen gauge.	19
14 – Three axis strain gauge used to determine strain in the substrate.	20
15 - ASTM E837 Residual Stress Determination Drilling Apparatus	21
16 - Results for Aluminum Almen Strip exposed to 30 psi stream for 20 seconds	22
17 - Illustration of Hertzian Contact Force between two spheres.....	23
18 - Hertzian Contact Force between a sphere and a flat plate.....	24
19 - Panel 1 prior to shot peening	26

LIST OF FIGURES

Figure	Page
20 - Panel 1 after shot peening for 1 second/ 1 pass with S280 shot with a 1/2" nozzle and a 30 psi pressure setting.....	27
21 - Vector plot of panel 2 prior to shot peening.....	28
22 - Vector plot of panel 2 after exposure to a 30 psi shot stream from a 1/2" nozzle for 1 second/pass	29
23 - FEA result for a 1 second 30 psi panel.....	30
24 - Vector plot of Panel 3 prior to shot peening.....	32
25 - Panel 3 vector plot after 15 second exposure at the 30 psi setting with a 1/2" Nozzle	33
26 - Vector plot of panel 4 prior to shot peening.....	34
27 - Panel 4 vector plot after 15 second exposure at 30 psi setting with 1/2" Nozzle.....	35
28 - FEA results using data from, 20 second exposure at 30 psi, residual stress measurements..	36
29 - Vector plot of panel 5 prior to shot peening.....	37
30 - Vector plot of laser scan of panel 5 following exposure to a 30 psi shot stream from a 1/2" nozzle for 30 seconds/passes	38
31 - Vector plot of laser scan of panel 6 prior to shot peening.....	39
32 - Vector plot of laser scan of panel 6 after exposure to a 30 psi shot stream from a 1/2" nozzle for 30 seconds/passes	40
33 - Results of FEA shell model using residual stress data from an almen strip exposed to a 30 psi shot stream from a 3/8" nozzle for 35 seconds/passes	41

LIST OF TABLES

Table	Page
Table 1 – Comparison of Shot Peened Panels and FEA model	42

LIST OF ABBREVIATIONS / NOMENCLATURE

ASTM	American Society of Testing and Materials
FEA	Finite Element Analysis
BHN	Brinell Hardness Number

LIST OF SYMBOLS

V	Volume
W	Work
B	Work needed to create a unit of volume (Brinell Hardness Number)
D_i	Indent Diameter
D	Shot Diameter
E	Energy
M	Mass
v	Velocity
ρ	Density
P	Efficiency (The Fraction of Energy actually used to do Work)
E	Coefficient of Restitution
F	Force
A	Area
h	Depth of indent
R	Radius of Shot ($D/2$)
a	Difference between R and h

CHAPTER 1

1 INTRODUCTION

1.1 Background

Shot peening is the process of hitting the surfaces of a piece of metal with a stream of small, hard particles, called shot. The impact of the shot with the substrate induces compression stresses on the surface of the work piece. This action, shown in Figure 1, can be used for cleaning the surfaces of metal objects. It has even been proven to protect against stress corrosion cracking (ASM International Handbook Committee, 1994). However, for a long time, the primary purpose for shot peening has been to improve fatigue strength. The compressive stress induced on the surface of the metal parts by shot peening is very effective in mitigating the tensile stresses which initiate cracking. There are many applications for shot peening. However, we will concentrate on the deformation caused by inducing these surface stresses, to form aluminum sheet. This process is also referred to as contour forming.



Figure 1 - A shot stream from a nozzle impacts a strip of metal (ceramics.org)

The shot peening process is controlled using the following parameters: Intensity and Coverage. Intensity is measured, independent of a component's properties, using the standard Almen Strip, (SAE J443, 2010). Coverage is dependent solely on the component and the number of indents per unit area, (SAE J2277, 2009). The common element to both of these parameters is indent size. Increasing indent size will increase both intensity and coverage per shot. Almen Strip intensity measurement is done per SAE J442 (Nov 2008): The material for the Almen strip is SAE 1070 Cold Rolled Spring Steel.

1.2 Literature Review

Many studies of shot peening have been conducted over the years. (Meguid S. S., 1999) modeled co-indenting using rigid shot impacting a substrate with two symmetry boundary conditions. This study showed that the proximity of simultaneous impacts had a significant influence on the stresses induced. (Klemen, 2009) simulated multiple ordered impacts using an isotropic-kinematic hardening law to model the behavior of AISI 4140 steel. Their constitutive law took into account both strain history and strain rate. Good correlation was observed between experimental data and simulation results for surface deformation and residual stresses. (Guagliano, 2001) used fatigue properties and work hardening to model multiple load cycles during multiple impacts on a SAE 1070 steel target. Schwarzer et al. (2002) suggested a 3D geometry to study the effect of multiple steel shots impacting an AISI 4140 steel target. This study modeled the shot with rigid surfaces and mass and rotary inertia elements. They also used infinite element models to reduce stress wave energy reflection into the mesh and residual stress profiles were averaged over an area covering multiple impacts. They also evaluated differences between successive and simultaneous adjacent impacts.

Meguid et al. (2002) introduced a symmetry cell representing successive rows of steel shot impacting a large AISI 4340 surface. Mass and stiffness damping were used. Shot deformation was studied and rigid elements were chosen to represent the shot. The effect of friction on the plastic strain induced was determined negligible for coefficients of friction between 0.25 and 0.5. Wang et al. (2002) proposed using random impacts to simulate the shot peening process. Miao et al. (2009) suggested a random finite element model and showed that this type of model could be used to study the influence of peening parameters on residual stresses, saturation, coverage, and surface roughness.

Zimmermann et al. (2010) compared deterministic and random finite element simulations regarding the development of coverage, residual stresses and surface topography. Using a strain rate sensitive isotropic-kinematic hardening law for Inconel 718, decent predictions of residual stress profiles were developed. Using a symmetry cell, Kim et al. (2010) showed that averaging calculated stresses over an impacted area provides results closer to experimental x-ray diffraction measurements of residual stresses than a 4-node average. Kang et al. (2010) modeled single and multiple predefined impacts of steel shots on a square 2024-T351 target. A spring back static analysis was used to stabilize the model. The authors showed that multiple impacts tend to create a uniform state in the peened material and that multiple impact modeling is more appropriate than single-impact models to represent shot peening and peen forming. Numerical tools have also been developed for forming simulation. These tools use equivalent loading methods to determine deformed shapes of large parts without simulating millions of impacts.

Grasty and Andrew (1996) introduced a “squeezed-layer” model: by applying a squeezing pressure causing yielding of surface elements, permanent deformations and a stress distribution were obtained. Successive loading cycles were applied to determine a stabilized deflection.

Calibration was however required to find the appropriate squeezing pressure. Levers and Prior (1998) suggested a thermal loading method to simulate peen forming processes. Their method consisted of introducing stress distributions in shell elements by creating thermal strains. Wang et al. (2006) suggested a thermally-applied loading unit to create a plastic layer in shell elements. The case of unconstrained peening, in which the sample is free to bend and elongate, was studied. A numerical arc height vs. peening time curve was obtained by applying multiple loading cycles and, with proper calibration, accurate predictions were obtained. It should be noted that in the models of Levers and Prior (1998) and Wang et al. (2006), temperature was used as a numerical tool and was not related to the actual process.

Han et al. (2002) proposed an equivalent loading scheme that used induced stresses in a solid model to simulate peen forming. Experimental research on shot peening and peen forming has also been performed. Cao et al. (1995) studied the progressive deformation of an Almen strip in an Almen holder during peening in multiple passes. They observed non-uniform curvatures in the constrained and free Almen strip. The authors proposed an analytical model to explain this behavior. X-ray diffraction was used to profile residual stresses after various numbers of passes. Miao et al. (2010) performed a detailed study on the peening of aluminum strips and plates. They studied the effects of shot velocity on saturation, roughness, and coverage and obtained residual stress profiles in thin and thick peened samples. The authors also measured monotonic mechanical properties of 2024 and studied the effect of material anisotropy on the development of arc heights. (Garipey, Larose, Perron, & Levesque, 2011) proposed the use of a shell element model using stresses determined using dynamic FEA models.

As a result of this literary review, it seems there has not been a study that uses the most reliable method of measuring residual stresses beyond the surface of a substrate (Vishay, 2010),

the hole drill method. It also seems the use of shell elements to represent different layers of stresses throughout a shot peened sheet has yet to be implemented as a practical and easy way to correlate shot peen intensity to arc height/distortion.

1.3 Objective

The objective of this thesis is to simulate the deformation due to the residual stresses induced by shot peening on an aluminum substrate. The Finite Element Method is well established method for analyzing linear deformation. However, the use for non-linear deformation is growing in manufacturing plants. The physics involved have been shown to be reliable through energy equations and their like since the time of Sir Isaac Newton. This research shall demonstrate that the use of empirical data and FEA can supply pragmatic solutions to many manufacturing issues found to this day.

CHAPTER 2

2 METHODOLOGY

2.1 Specific Tasks

This thesis is formed on the application of empirical data to a small number of sets of shell elements to evaluate or predict the deformation that will be seen in a substrate. Using dynamic models to recreate the millions of pieces of shot impacting a substrate would be incredibly computationally expensive. This research explores the use of dynamic contact models and the use of data reduction in a simplified shell model to demonstrate the simple application of empirically determined stresses to shell elements in a quasi-static 3D model can produce predictive models of the deformation that will be seen in a substrate.

This research aims to establish the method by which shot peen deformation can be predicted by following these steps:

1. Shot peen “Almen Strip” sized specimens of the same alloy to be formed.
2. Take residual stress measurements for varying intensities and exposures.
3. Identify characteristic stresses for each exposure and intensity.
4. Apply the representative characteristic residual stress to shell elements in an FEA model.
5. Use the deformation in the model to guide shot peening to generate parts with the desired contour.

2.2 Analytical Calculations

2.2.1 Volume of an Indent

Kirk has written extensively about shot peening. In his paper, how indent diameter ties the two main parameters, intensity and coverage, of shot peening together are explained (Kirk, 2004). Determination of the volume of an indent is described accordingly.

The volume (**V**) of the indent can be described by the following simple Equation:

$$\mathbf{V}=\mathbf{W}/\mathbf{B} \quad (1)$$

where: **W** is the work done by the shot, and **B** is work needed to create a unit of volume.

The hemispherical indent volume **V** of a spherical shot is given by the following equation:

$$\mathbf{V} = \pi\mathbf{D}_i^4/32\mathbf{D} + \pi\mathbf{D}_i^6/64\mathbf{D}^3 \quad (2)$$

For simplification, we shall ignore the small contribution of the second term and use:

$$\mathbf{V} = \pi\mathbf{D}_i^4/32\mathbf{D} \quad (3)$$

where **D_i** is the indent diameter and **D** is the shot diameter. An example of this type of shot peening is depicted in Figure 2.

2.2.2 Energy and Work

The energy (**E**) in a shot particle is provided using the kinetic energy relation:

$$\mathbf{E} = \frac{1}{2}\mathbf{mv}^2 \quad (4)$$

where **m** is the mass and **v** is the velocity.

$$\mathbf{Mass} (\mathbf{m}) = \mathbf{V} \cdot \rho \quad (5)$$

where **ρ** is the density of the shot particle.

Substituting the equation for mass (equation 5) into the kinetic energy equation (equation 4), one obtains:

$$E = \pi D^3 \rho v^2 / 12 \quad (6)$$

A fraction, **P**, of the kinetic energy, **E**, is used as the work, **W**, needed to create the indent in the component. The rest of the energy is retained by the shot and is indicated by the coefficient of restitution, **e**.

$$P = (1 - e^2) \quad (7)$$

where from kinetic energy considerations before and after shot impact, it can be evaluated as,

$$e^2 = \text{height of bounce} / \text{Drop height} \quad (8)$$

Using equation 6 for the energy of the shot, the work done by the shot can be determined as,

$$W = P \cdot E = P \pi D^3 \rho v^2 / 12 \quad (9)$$

And substituting the equation for the fraction of work done based on the coefficient of restitution, the work done by the shot can be calculated as,

$$W = (1 - e^2) \pi D^3 \rho v^2 / 12 \quad (10)$$

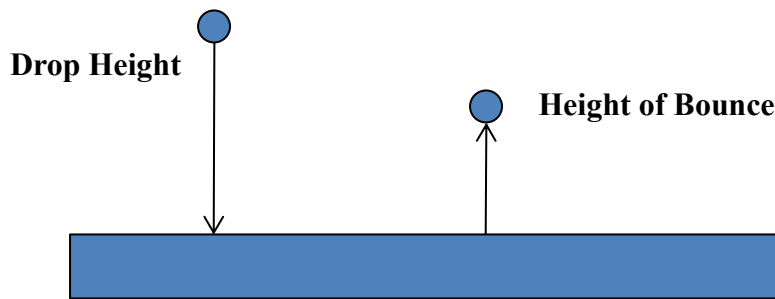


Figure 2 – The work done to the substrate is observed in the difference between the drop height and the height of the bounce of the shot

2.2.3 Brinell Hardness Number

The Brinell Hardness Number (BHN) can also be considered as the amount of work per unit volume of indent, measured in kilograms of force per square millimeter. Obviously, the indent left by a single spherical shot is not a cylindrical shape. However, it is much easier to compute the volume of a cylinder. Therefore, we will simplify the calculation of work done per unit volume by estimating it to be a simple cylindrical shape as illustrated in Figure 3. The force, F , during indentation is initially zero and builds up linearly with increasing indentation depth until it reaches a maximum, F_{\max} . The average force during indentation is therefore $F_{\max}/2$ so that the work done is $F_{\max} \cdot h/2$. Where h is the depth of the indent. The indent area also varies from zero (on initial contact of sphere and component) to a maximum, say A , with the average indent area being $A/2$. The volume of the indent is therefore given by $A \cdot h/2$. Dividing the work done by volume of indent is then simply F_{\max}/A , which is the Brinell hardness number, $BHN=B$.

$$B = BHN = \frac{\text{Load on indenting tool (Kgf)}}{\text{Surface area of indentation (mm}^2\text{)}} \quad (11)$$

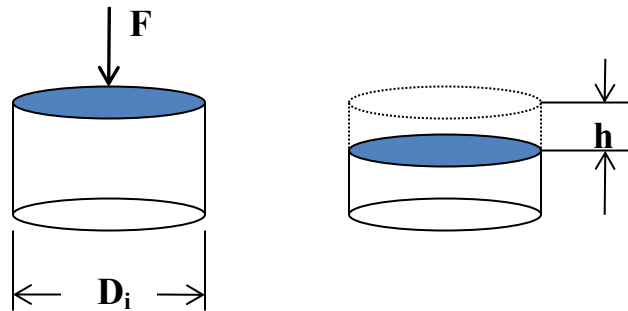
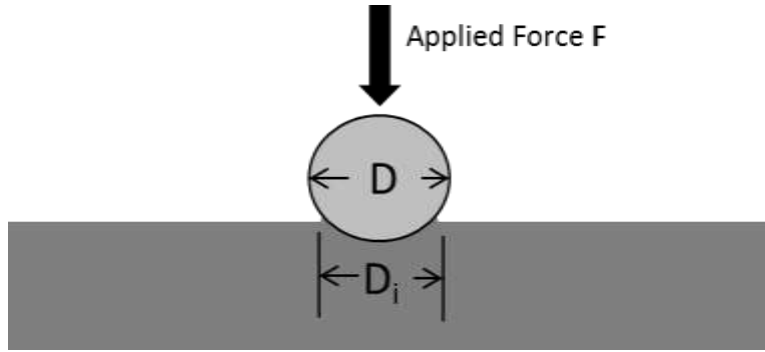


Figure 3 - Work done per unit volume is simplified by calculating the compression of a representative cylinder.

The Brinell Hardness Number (BHN) for SAE1070, the material used for Almen Strips is:

192Kgf/mm² [Kilograms Force/ mm²] (MatWeb, 2013) as shown in Figure 4.



$$\text{BHN} = \frac{F}{\frac{\pi}{2}D \cdot (D - \sqrt{D^2 - D_i^2})} \quad (12)$$

Figure 4 - Brinell Hardness Number

By inputting this information into the equation for the volume of the indent it is possible to derive the indent diameter:

$$V = W/B = \pi D_i^4 / 32D = (1 - e^2) \pi D^3 \rho v^2 / 12/B \quad (13)$$

Solving for D_i gives:
$$D_i = 1.278D(1 - e^2)^{.25} \rho^{.25} v^{.5} / B^{.25} \quad (14)$$

2.2.4 An Illustrative Example

Consider an S170 Steel shot and 2024-T3 Aluminum as a target.

Shot: **Diameter (D) = .0165" or .425mm** and a density of $\rho = 0.284 \text{ lb/in}^3$ ($\sim 7860 \frac{\text{kg}}{\text{m}^3}$)

The initial velocity is given to the shot is $v = 1575 \frac{\text{in}}{\text{s}}$ ($\sim 40 \frac{\text{m}}{\text{s}}$)

Assume $e = .5$, and therefore $P = (1 - e^2) = .75$

In order to convert kg/mm^2 to N/m^2 (Pa) it is necessary to multiply by 9.8×10^6 ; hence,

$$\text{BHN} = 120 \frac{\text{Kgf}}{\text{mm}^2} \times 9.8 \times 10^6 = 1.18 \text{GPa (Matweb)}$$

$D_i = .0065 \text{in} \sim .165 \text{mm}$ as shown in Figure 5.

Hence, the indentation diameter D_i can be evaluated.

$$D = .0165''$$

$$D_i = .0065''$$

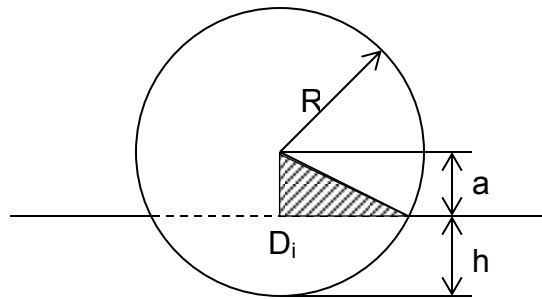


Figure 5 - Geometry of an indent

For, calculating the depth of the indent, the Pythagorean Theorem can be used as shown in Figure 5.

Assuming the radius of the indent is equal to that of the indenter or shot, we conclude,

$$h = R - a$$

$$a = \sqrt{R^2 - (D_i/2)^2}$$

$$a = \sqrt{.00825^2 - .00325^2} = .00785 \text{ inch}$$

$$h = .00825 - .00785 = .0004 \text{ inches or } \sim 0.01 \text{ mm}$$

Hence, these calculated dimensions were used to evaluate the following dynamic models.

2.3 Dynamic Modeling

Having used the calculations described in chapter one, the first step was to build a model to that correlated the calculations with an FEA model. Using MSC Marc Mentat, a dynamic contact model was built using Hex-mesh for a sphere and a prism. These represented a single shot and the substrate being shot peened, respectively. A picture of the indent result of the first model can be seen in Figure 6. However this explicit model took many hours to run and the probability that this could be used to determine deformation in a timely manner was apparent.

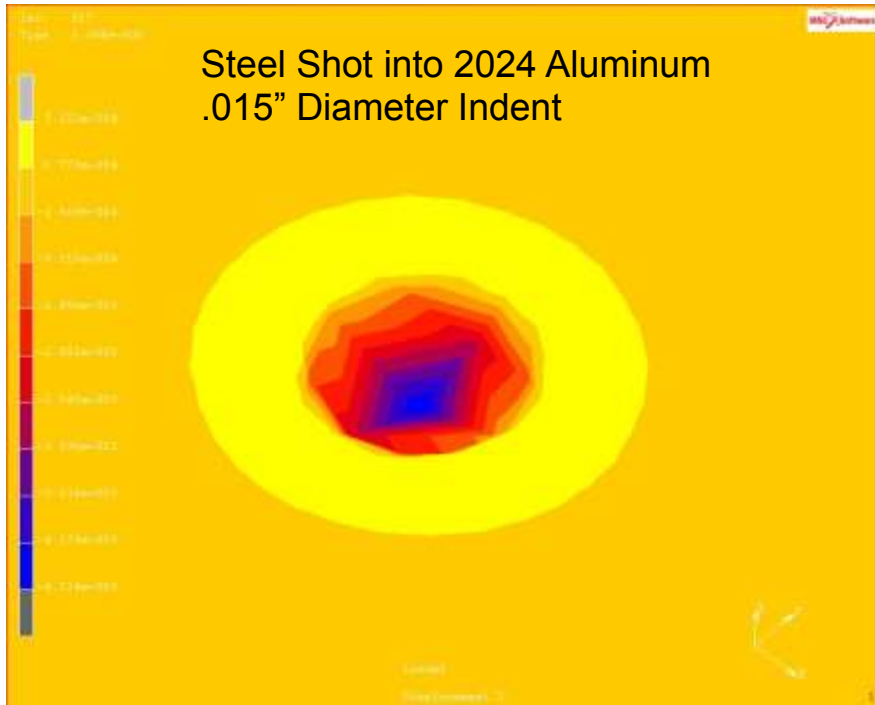


Figure 6 - Results of dynamic analysis using MSC Marc Mentat to model the shot and aluminum plate.

The dynamic model used a 3D, 8 node, Hex-mesh, full-integration element (Element 7, MSC Marc Mentat, 2010) for both the spherical shot and aluminum substrate. The substrate was modeled using a 10x10x10 element cube. An aspect ratio of 1 (equal length sides were used for all elements) resulted in a 0.050 inch cube. The 36 elements constituting the shot contact body, were shaped to approximate a sphere. Symmetry planes were used on the length and width of the model. These symmetry lines held the shot centered on the substrate throughout the impact and guaranteed node to node contact. The substrate was also fixed in the Z-axis (thickness) by the nodes making up the bottom surface. The shot was given an initial velocity of 40m/s normal to and heading toward the substrate. The initial position was only a few thousandths of an inch above the substrate to save the computation of the flight of the shot.

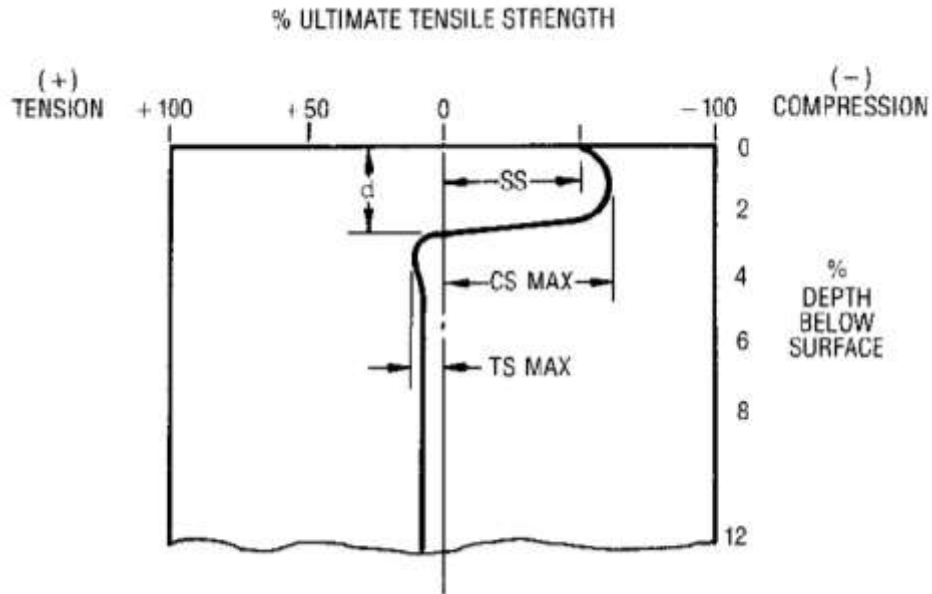


Figure 7 - Graph showing the expected stress distribution through the thickness of a shot peened surface. (Champaign, 2001)

Figure 5 shows the expected distribution of stresses in a substrate due to shot peening. The 3D dynamic model was evaluated to see if the same type of distribution was apparent in the FEA model. MSC Marc Mentat allows the user to evaluate the stress at different locations using a node path. A picture of the symmetric model can be seen in Figure 8 below. As observed in Figure 8, the highlighted nodes indicate the node path for the graph of stresses shown in Figure 9.

The symmetric dynamic model shown in Figure 8, was modeled using hexagonal mesh for the substrate and shot. The substrate was made up of fifty, 0.005" cubes, and the 0.028" diameter shot was made up of 36 hex elements arranged as seen in Figure 8. The shot was given an initial velocity of 40 m/s in the direction of the substrate on a vector normal to the surface. The results, shown in Figure 6 shows that the model, using the proper material properties and identical initial conditions, was able to closely recreate the manually calculated results. Differences are possible due to model parameters, such as mesh size of each the sphere and substrate models. However, for a fully correlated model, the size of the mesh may be changed or

the properties of the materials may be adjusted to match the calculated or empirical tested results. Dr. Kirk discussed factors that might influence the deformation seen in a substrate. (Kirk, Fall 2009)

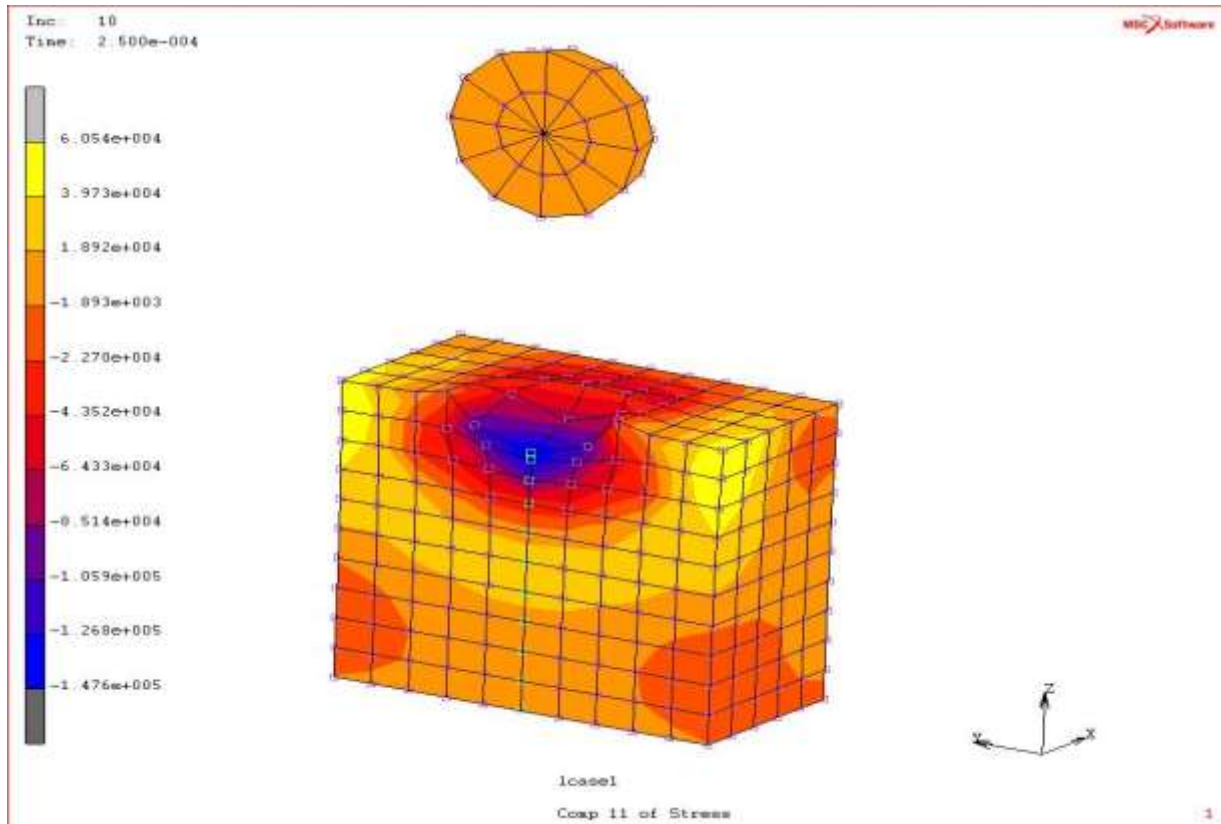


Figure 8 - Symmetric model of single shot and a section of an aluminum plate. Modeled using MSC Marc Mentat.



Figure 9 - Graph of the results of the FEA model. Components of the residual stress through the thickness of the part is compressive near the surface and the tensile residual stress deeper below the surface.

The data from the dynamic FEA model shows the expected mode shape for the stress curve. Figure 9 shows compressive stress near the surface that was impacted by the shot, and the tensile stresses deeper in the substrate. The mesh was set up with 10 elements through the thickness of the representation of the substrate. This coarse mesh may explain why the compressive stress appears to propagate deeper into the substrate than expected. For future studies it is recommended that a finer mesh be used to get a better representation of the depth of the compressive stress. This study however, concluded that the dynamic model was not practical for determining deformations due to shot peening. The information to demonstrate the challenges of relying on mathematical models and the advantages of using empirical data, however, were included in this thesis.

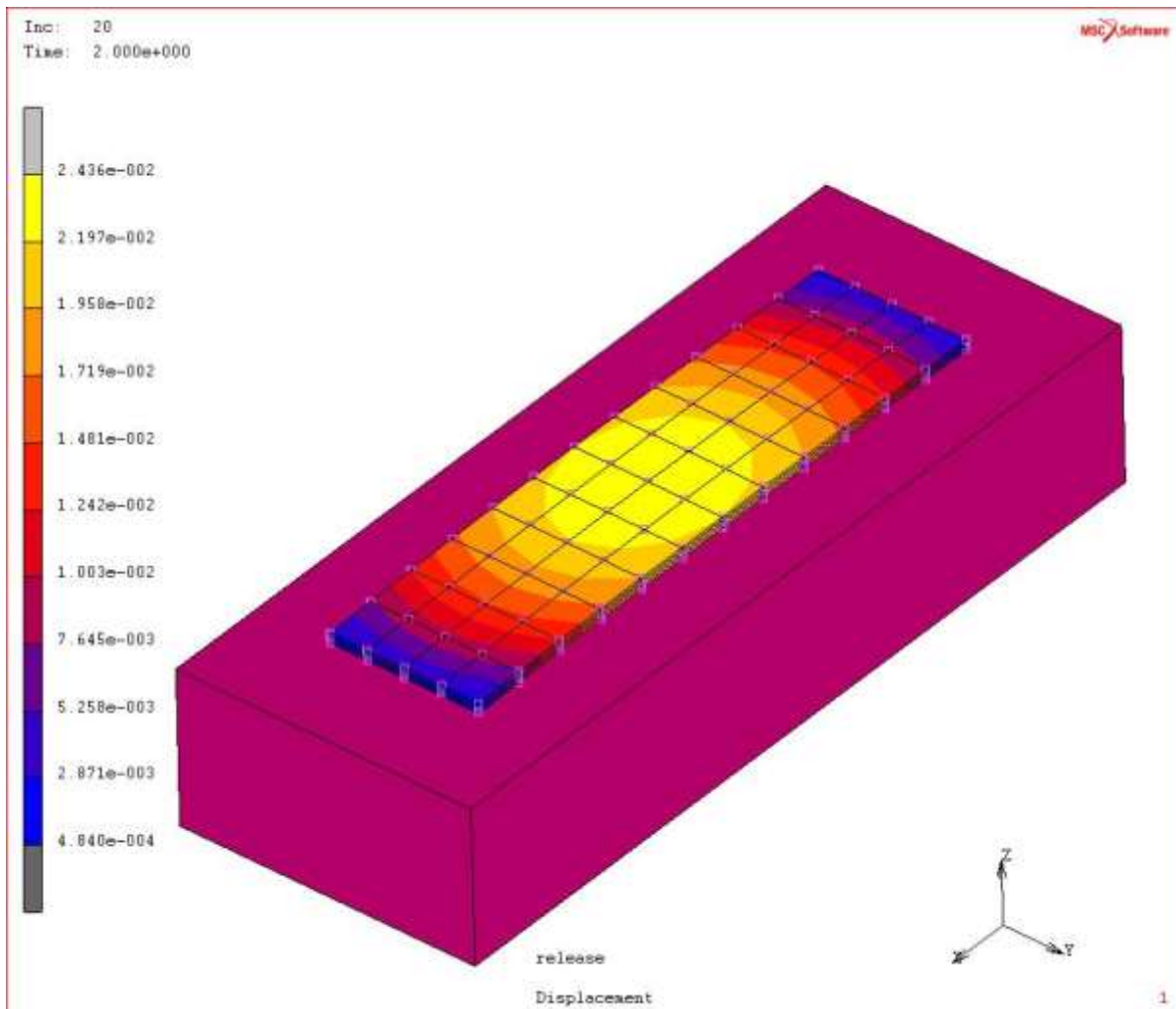


Figure 10 - Results showing the displacement of an aluminum almen strip with residual stresses measured using the hole drill method.

To avoid the computational expense of using a dynamic impact model, it was determined that simply inputting the residual stresses measured from a shot peen test sample would produce deformation similar to what is seen in reality. Figure 10 shows an example of one such model where the stresses measured using the hole drill method were used to produce deformation in an FEA model.



Figure 11 - Steel Almen strips on the left and Aluminum Almen Strips on the right, labeled with exposure time and arc heights measured in ten thousandths of an inch.

2.4 Shot peening

7075-T6 bare aluminum was cut it into Almen strip sized pieces and shot peened using increasing amounts of pressure in a manual shot peen process. For each machine pressure setting we exposed the strips for increasing amounts of time. Figure 11 shows the results for the 30 psi machine setting. This results in an intensity of 67, the arc height of a standard Almen strip made from 1070 cold rolled steel at the point of saturation. Saturation is defined as the point at which the arc height increases by less than 10% when you double the exposure.

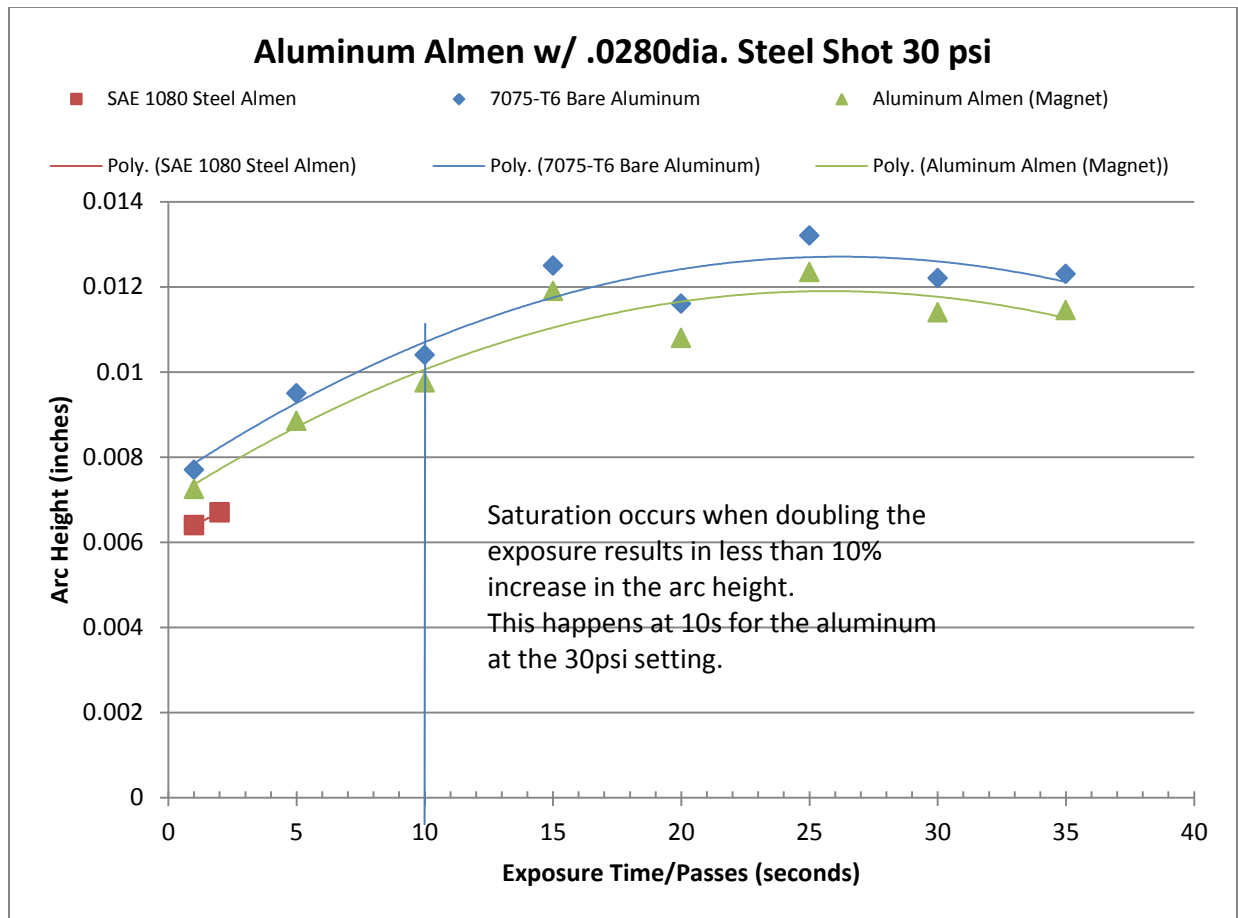


Figure 12 - Graph of the Arc Height of the 7075-T6 strips vs the exposure time/passes.

It can be seen in Figure 12 that the saturation point for the aluminum strips occurs after 10 seconds of exposure resulting in an arc height of .0104". It is also interesting to note that the maximum arc height seems to occur at 2.5x the saturation point. Over peening is an issue that needs to be addressed when shot peening. However this subject can be left to other studies for now.

The two lines representing the arc height of the aluminum strips are comprised of two different measuring methods. The first measurements were made by the shot peen operator, Elmer, by placing the almen strip block on top of the strip to hold it on the gauge. The second line of measurements was made using a flexible magnet that laid on top of the aluminum strip and together with the magnets on the almen strip gauge held the aluminum strip in place for

measurement. You can see in Figure 12 that the overall magnitude of the measurements was different but the relative magnitudes between measurements remained fairly constant.

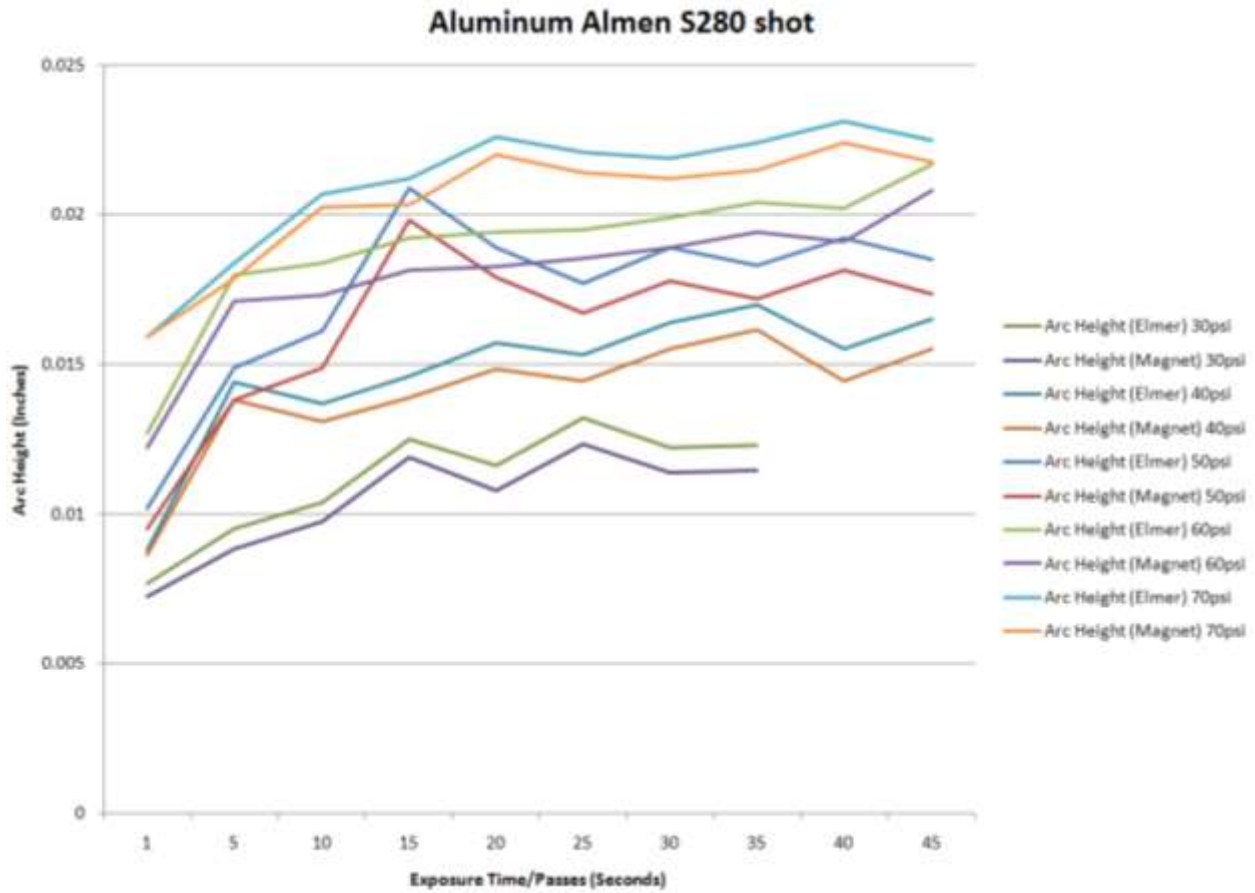


Figure 13 - Exposure Time/Passes vs. Arc height as measured manually by Elmer and using a Magnet to hold the strip in an Almen gauge.

Figure 13 shows the summary of all the results gathered for different air pressures used to accelerate the S-280 steel shot. This makes it easy to identify the effect of higher air pressure on the intensity seen on the aluminum strips. Although saturation occurs at roughly the same exposure time, the arc height (intensity) increases with the greater air pressure (higher energy) and therefore more cold work done by the shot peening process. Greater arc height is associated with greater strains and therefore higher residual stresses in the substrate.



Figure 14 – Three axis strain gauge used to determine strain in the substrate.

The actual residual stresses induced into the aluminum almen strips were measured using the apparatus shown in Figure 14. The precision drilling guide is shown in Figure 15. The aluminum strip was held in place using a sealant to adhere it to a larger plate. Per ASTM E837, the Type A strain gauge affixed to the strip indicated the strain exhibited in the strip, as a hole was drilled incrementally into the strip.

The strain values were used with the modulus of the material to calculate the stress induced by the shot peening process using the standard relationship between strain and modulus.

$$\sigma = E\varepsilon \quad (15)$$

The actual calculations are a bit more complicated than that however. I will not go into them here, although details on how to determine the residual stresses using the hole drill method can be found in Vishay's manual on the topic. (Vishay, 2010) An Excel spreadsheet was made to calculate all the stresses for application in the FEA models used in this thesis.



Figure 15 - ASTM E837 Residual Stress Determination Drilling Apparatus

2.5 Measuring Residual Stress

The results of the testing provided results such as those shown in Figure 16 for all of the pressure settings and exposures tested. Once again the shape of the curve from the dynamic FEA model is validated with the expected stresses. These strains would be simulated using shell elements placed at the appropriate depth to recreate this distribution in the FEA model of the panel. We see the maximum compressive stresses occur between .004" and .010" below the shot peened surface. This measurement assumed zero stress at the top surface, however increments of .002" were used when drilling into the aluminum "almen" strip. We can see the strains produced by drilling stopped after .036" of depth and anything over .050" is obviously already through the .050" thick strip.

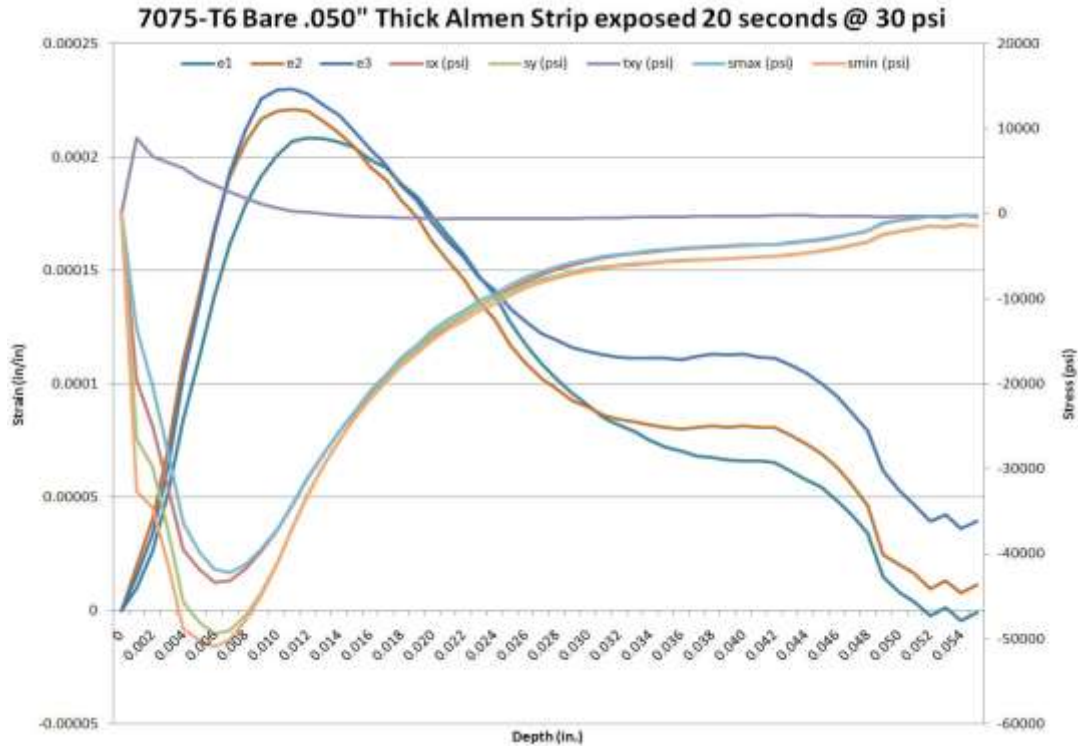


Figure 16 - Results for Aluminum Almen Strip exposed to 30 psi stream for 20 seconds

2.6 Quasi-Static Contact/Impact Modeling and Analysis

Hertzian Contact Force and the depth of an indent

Another computational approach to the impact problem includes Hertzian Contact Force.

(Shivaswami & Lankarani, 1997) Shivaswami and Lankarani have presented this quasi-static approach in their paper from 1997. It is noted that this computation is applicable only to situations with local deformation and not large deformation that might be seen in some other catastrophic impact event.

Hertzian contact force is based on an elastic type Hooke's law for impact/contact between two spheres as shown in Figure 17.

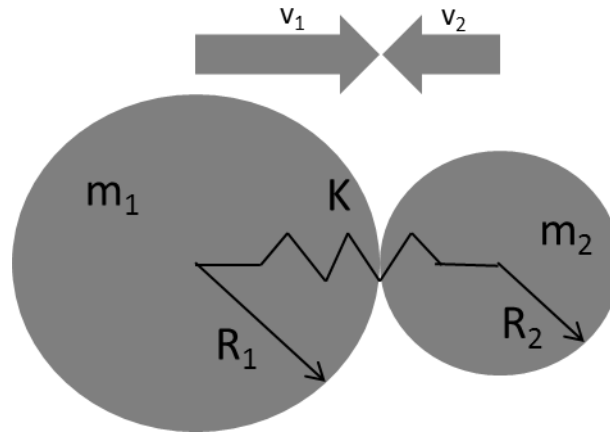


Figure 17 - Illustration of Hertzian Contact Force between two spheres

$$\mathbf{F} = \mathbf{K}\delta^n \quad (16)$$

where \mathbf{F} is the contact force, δ is the indentation, \mathbf{n} is a material dependent constant and \mathbf{K} is the contact stiffness, which can be evaluated as:

$$\mathbf{K} = \frac{4}{3\pi(\mathbf{h}_1 + \mathbf{h}_2)} \sqrt{\frac{\mathbf{R}_1\mathbf{R}_2}{\mathbf{R}_1 + \mathbf{R}_2}} \quad (17)$$

where \mathbf{h} is defined as:

$$\mathbf{h}_i = \frac{1 - \mathbf{v}_i^2}{\pi\mathbf{E}_i}; i = 1, 2 \quad (18)$$

and \mathbf{v} is Poissons ratio and \mathbf{E} is Young's Modulus.

For this study, \mathbf{R}_1 will be the radius of a single piece of shot, and \mathbf{R}_2 will be the radius of the plate that is being shot peen formed. Since the piece of aluminum we are shot peening is flat, we assume the radius to be infinite. This is obviously not completely true, since we are inducing curvature into the pieces of metal. However, the radius of the shot is orders of magnitude smaller than that of the substrate being shot peened and again making the assumption of infinite radius reasonable. This simplifies equation (17) as follows:

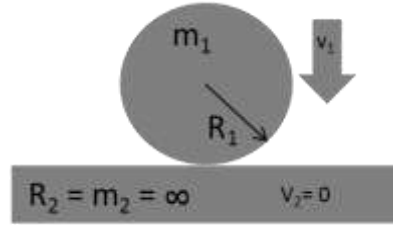


Figure 18 - Hertzian Contact Force between a sphere and a flat plate

$$K = \frac{4}{3\pi(h_1 + h_2)} \sqrt{R_1} \quad (19)$$

This stiffness is then used in the deflection equation to determine the maximum indent seen by the substrate as follows: (Shivaswami & Lankarani, 1997)

$$\delta_{\max} = \left[\frac{n+1}{2K} m_{\text{eff}} v^2 \right]^{\frac{1}{n+1}} \quad (20)$$

Applying the same assumption used for the radii, we simplify the equation for effective mass of the system by assuming m_2 is infinite. This results in the following equation for effective mass:

$$m_{\text{eff}} = m_1 \quad (21)$$

Substituting equation (21) into (20) we get:

$$\delta_{\max} = \left[\frac{n+1}{2K} m_1 v^2 \right]^{\frac{1}{n+1}} \quad (22)$$

From this we can derive the maximum contact force:

$$F_{\max} = K \delta_{\max}^n \quad (23)$$

Shivaswami and Lankarani concluded that n should be between 1.65 and 1.7 for aluminum and between 1.7 and 1.76 for steel. Since we're using a steel shot and aluminum plate we shall use 1.7. Assuming $n=1.7$, the velocity of the shot and the coefficient of restitution the depth of the permanent indent due to the impact of one piece of shot can be calculated using this equation (Shivaswami & Lankarani, 1997):

$$\delta_p = \frac{(n + 1)m_1 v(1 - e^2)}{2F_{max}} \quad (24)$$

Using the same values from our first example, in chapter 1, we have:

$$\delta_p = \frac{(2.7)2.65E - 6 \cdot 40(1 - 0.5^2)}{2 \cdot 22.1} = 5.44E - 7m \quad (25)$$

This is equal to about 0.0002 inch, and is considerably smaller than what was calculated in chapter 1. Therefore the assumptions used to find the depth of the indent in chapter one proved to be unfounded. The resulting indentation radius should be considered quite smaller than the radius of the shot.

CHAPTER 3

3 COMPARISON OF RESULTS AND DISCUSSION

3.1 Results from Hybrid FEA Simulations of Shot Peening

The laser scan shown in Figure 19 shows the distance to a datum plane for a sheet prior to peening. This same datum would be used to measure the distance the plate was deformed after peening. This particular sheet already had approximately .070” of deformation. This indicates that some residual stress may already exist in the panel from fabrication, sheering and/or handling.

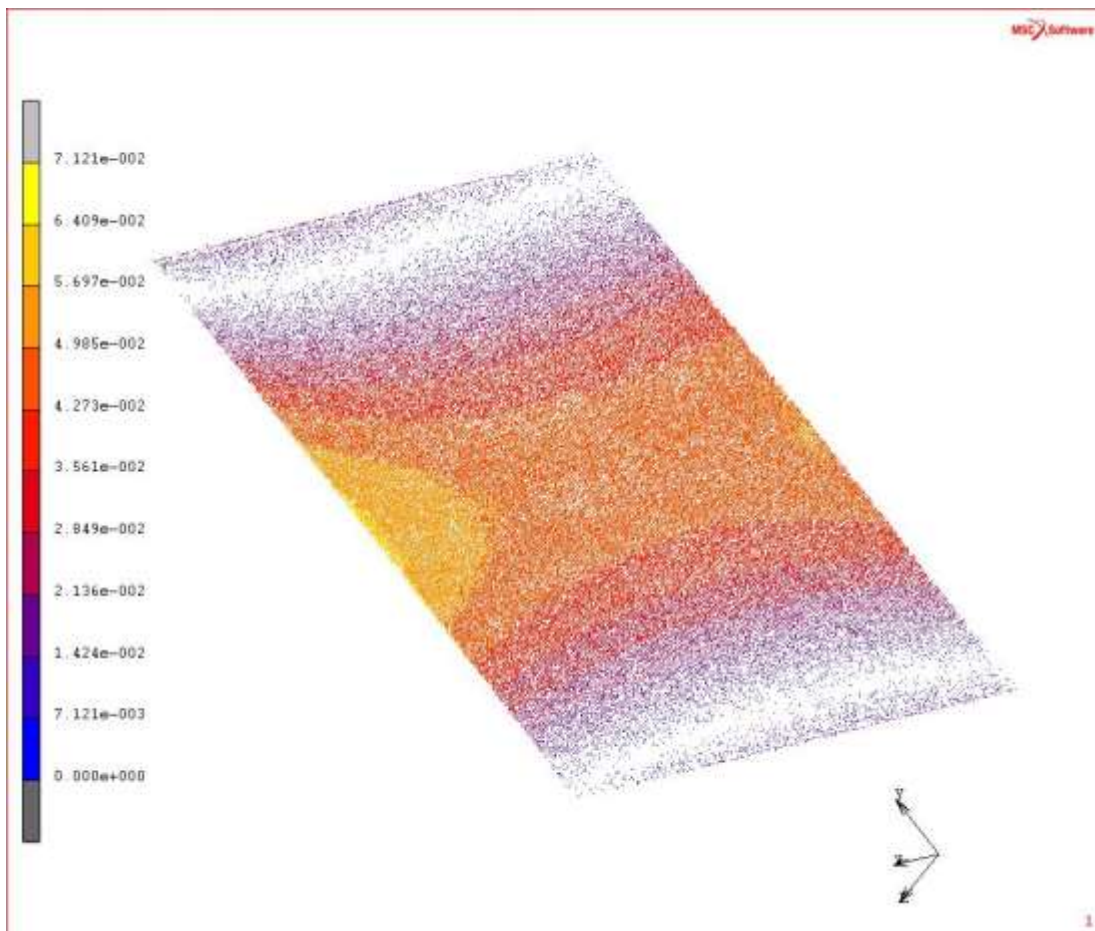


Figure 19 - Panel 1 prior to shot peening

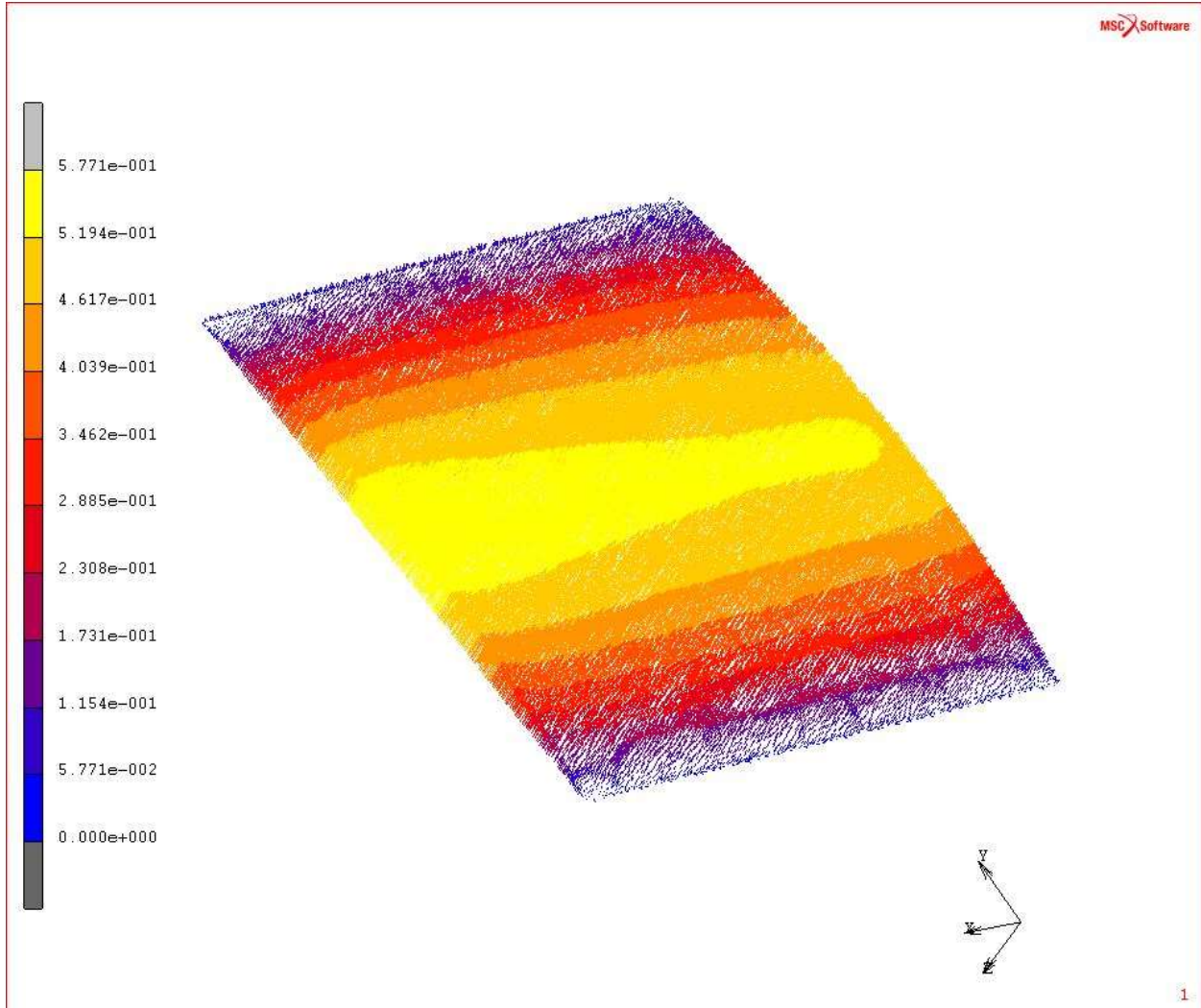


Figure 20 - Panel 1 after shot peening for 1 second/ 1 pass with S280 shot with a 1/2" nozzle and a 30 psi pressure setting

After shot peening, the aluminum panel was once again laser scanned. The points obtained were used to create the vector plot seen in Figure 20. The maximum deflection is shown to be 0.5771". This maximum was verified to be in the area where the laser scan of the pre-shot peened panel, Figure 19, displayed an initial offset of ~.070". This would suggest that using the initial deformation seen in the panel as part of the model, would lead to more accurate results.

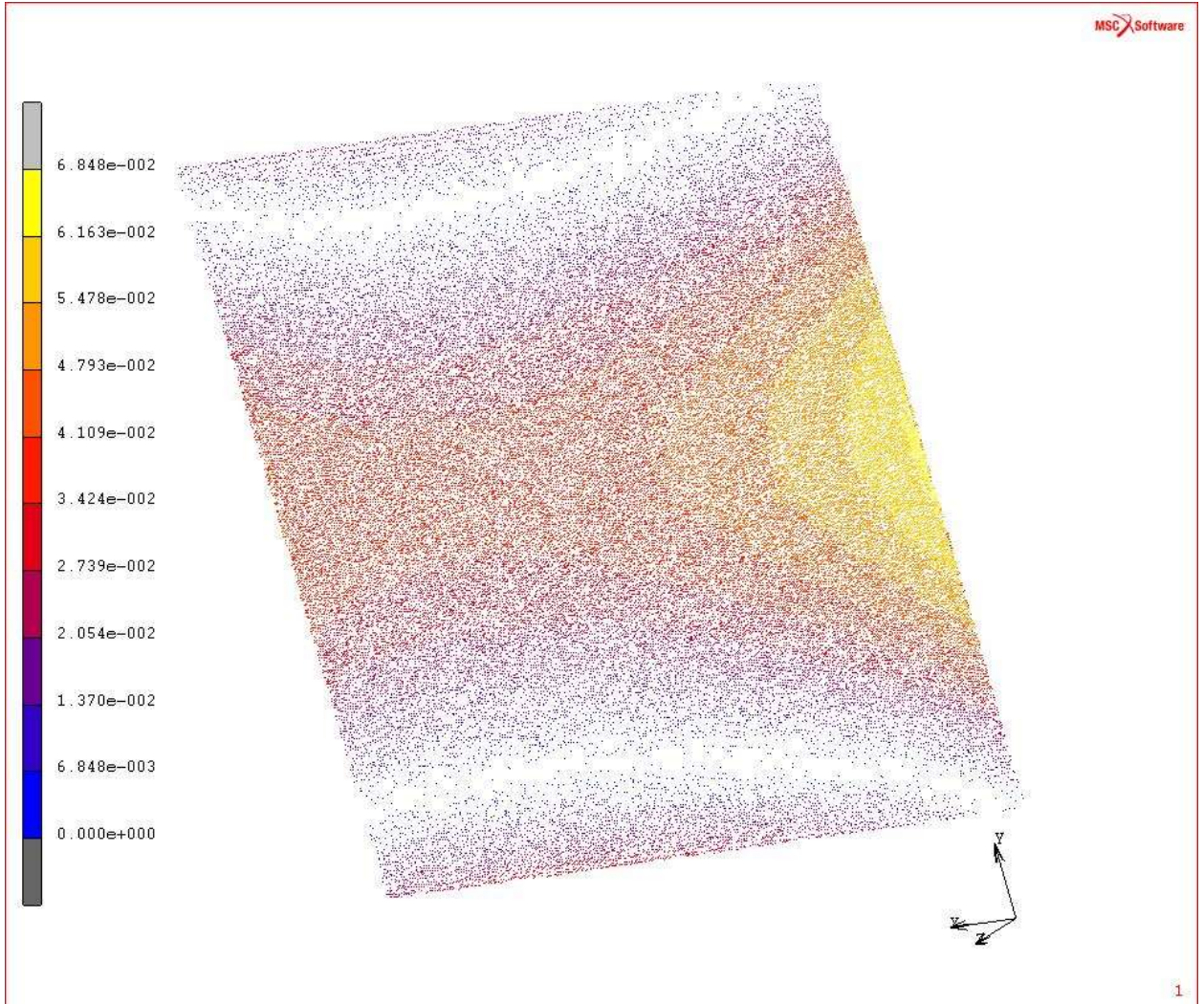


Figure 21 - Vector plot of panel 2 prior to shot peening

The second 10 inch x 10 inch panel, shown in Figure 21, also exhibited the initial out of plane displacement of approximately 0.070 inch. It can be shown that the area of maximum displacement is on the right of this panel as it is highlighted in yellow.

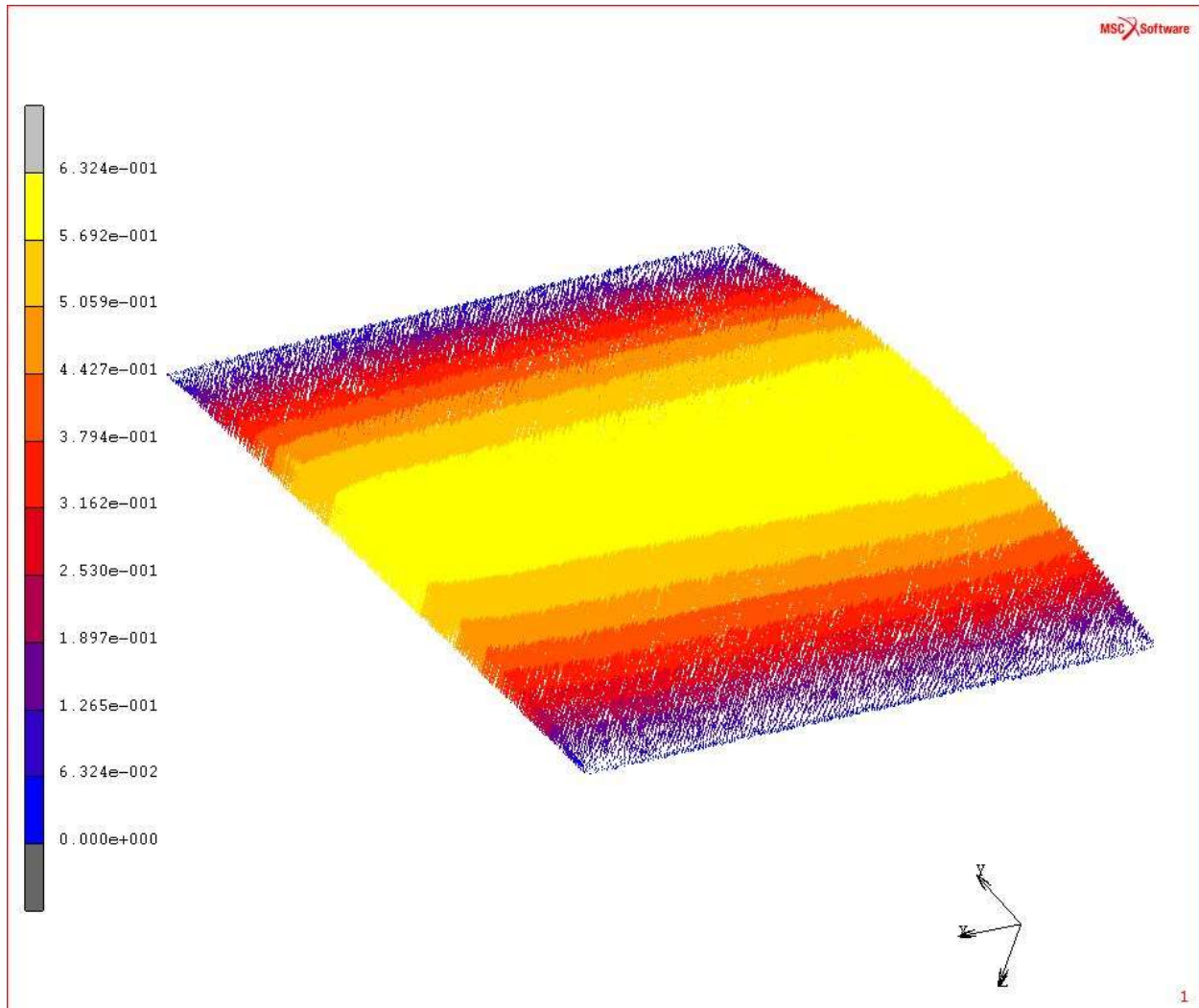


Figure 22 - Vector plot of panel 2 after exposure to a 30 psi shot stream from a 1/2" nozzle for 1 second/pass

After shot peening, panel 2 shown in Figure 22, still exhibits the maximum out of plane displacement at the right of the panel. This is again indicating that the residual stress induced by shot peening is additive to what already exists in the panel. It is important to keep the initial displacement found in the test panels when evaluating the FEA model. Also, keep in mind the FEA model starts with a perfectly flat panel.

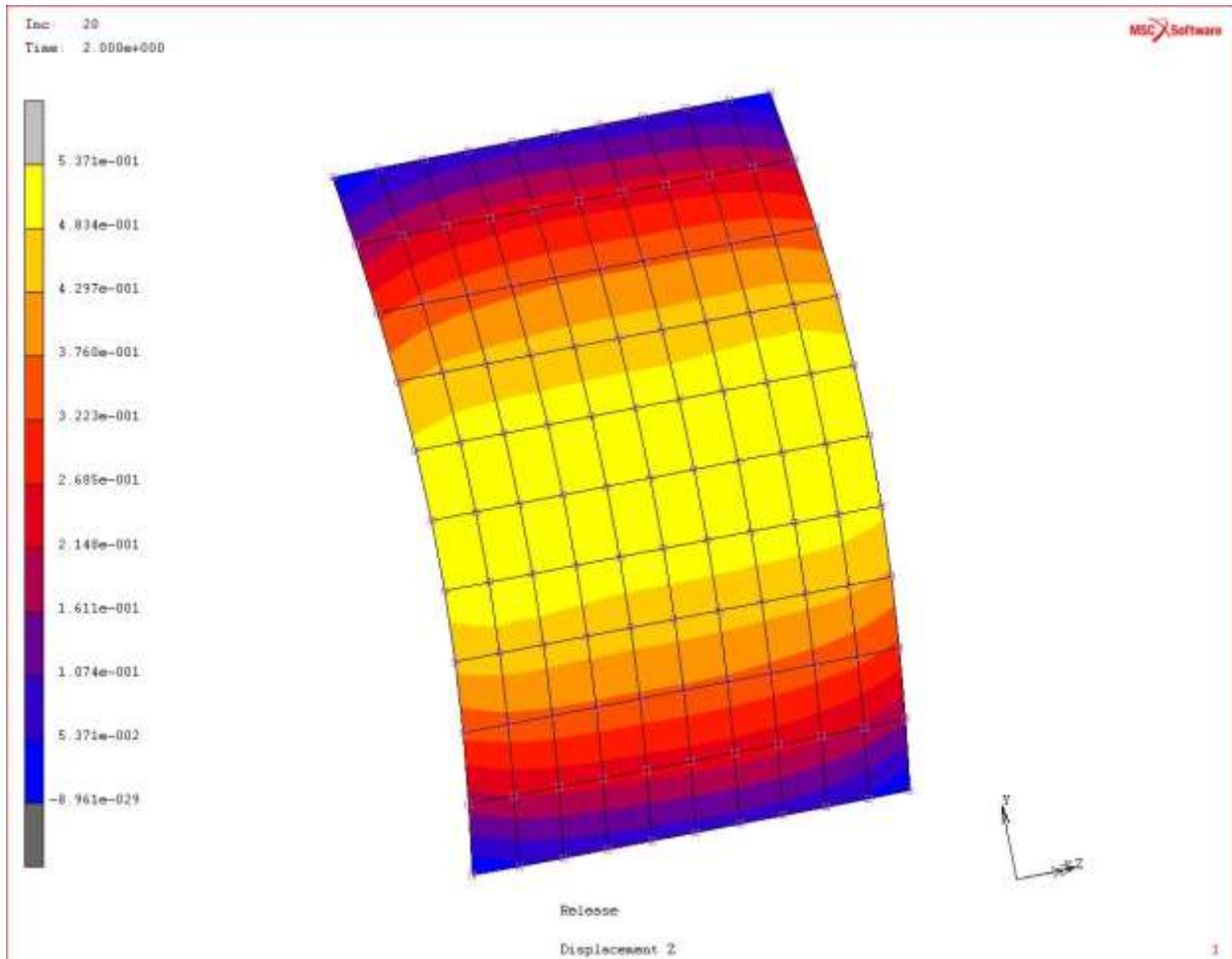


Figure 23 - FEA result for a 1 second 30 psi panel

The model of the aluminum panel uses the modulus of elasticity and a plasticity curve for 7075-T6 aluminum. Then the shell elements are given a thickness corresponding to the amount of depth that the shell layer represents. Each layer of shells is also offset to the appropriate distance from the surface that the shell layer represents. The average stress, over the thickness represented, is then applied to those shells. A shallow first layer of shell elements will simulate the average from the zero stress up until near the maximum compressive stresses induced by the shot. That maximum compressive stress will then be represented by shells at the depth from 0.004" to 0.010", as is the case in panel shown in Figure 16. Two more layers of shells

representing the average seen after the max and then the little to no strain areas passed the half way depth are used to represent the remainder of the thickness of the panel.

Symmetry planes were used through the middle of the length and width of the FEA panel. The most extreme nodes in the y-axis were held in the Z-axis during application of the initial conditions. A second loadcase was used to release all of these nodes except the corners of the plate. The corners were held to the plane used as reference for measuring arc height in the panels.

It is seen from using the empirical data, collected by drilling the aluminum strip that was shot peened for 1 second/pass of exposure, the FEA layered shell model produced a result very close to what is seen the 10x10 panels that were exposed to a shot stream for an equal amount of time. Differences exist in the two situations, however. It was noted during the collection of this data that the operator had used a 3/8" nozzle on the aluminum strips that were later drilled for exposures of 1, 20 and 35 seconds/passes. These 10x10 panels were shot peened using the same 30psi setting but with a 1/2" nozzle. This change in nozzle area certainly means the velocity and therefore the energy of the shot was different. It can safely be assumed the greater size nozzle would be associated with a lower velocity and therefore less energy and less deformation than what would be achieved with the smaller nozzle at the same pressure. Therefore, some variation should be considered for this difference.

The FEA model also starts from a perfectly flat condition, whereas the real sheet has some initial displacement. If the initial displacement is added to the FEA result it is extremely accurate. This initial displacement could be accounted for in future models by meshing the pre-shot laser scan of a specimen.

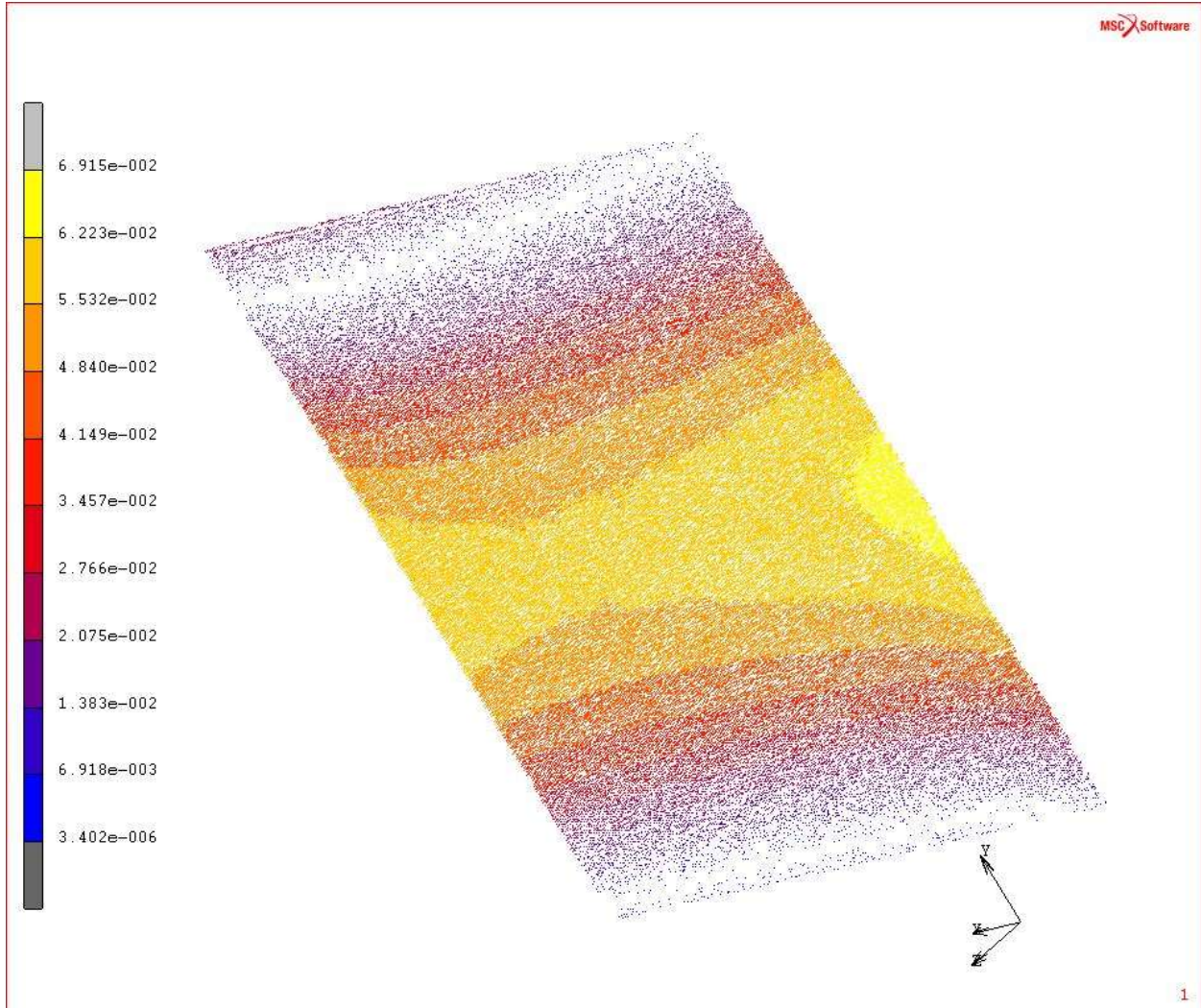


Figure 24 - Vector plot of Panel 3 prior to shot peening

Figure 24 shows the laser scan for the third panel. It also exhibits the 0.070 inch initial out of plane displacement in the third panel prior to shot peening. Note the hour glass shape of the contour and compare it to the shape seen in Figure 25. We can safely conclude the data in these two vector plots, is rotated 180°, due to the larger end of that hour glass shape being on opposite side of the figure.

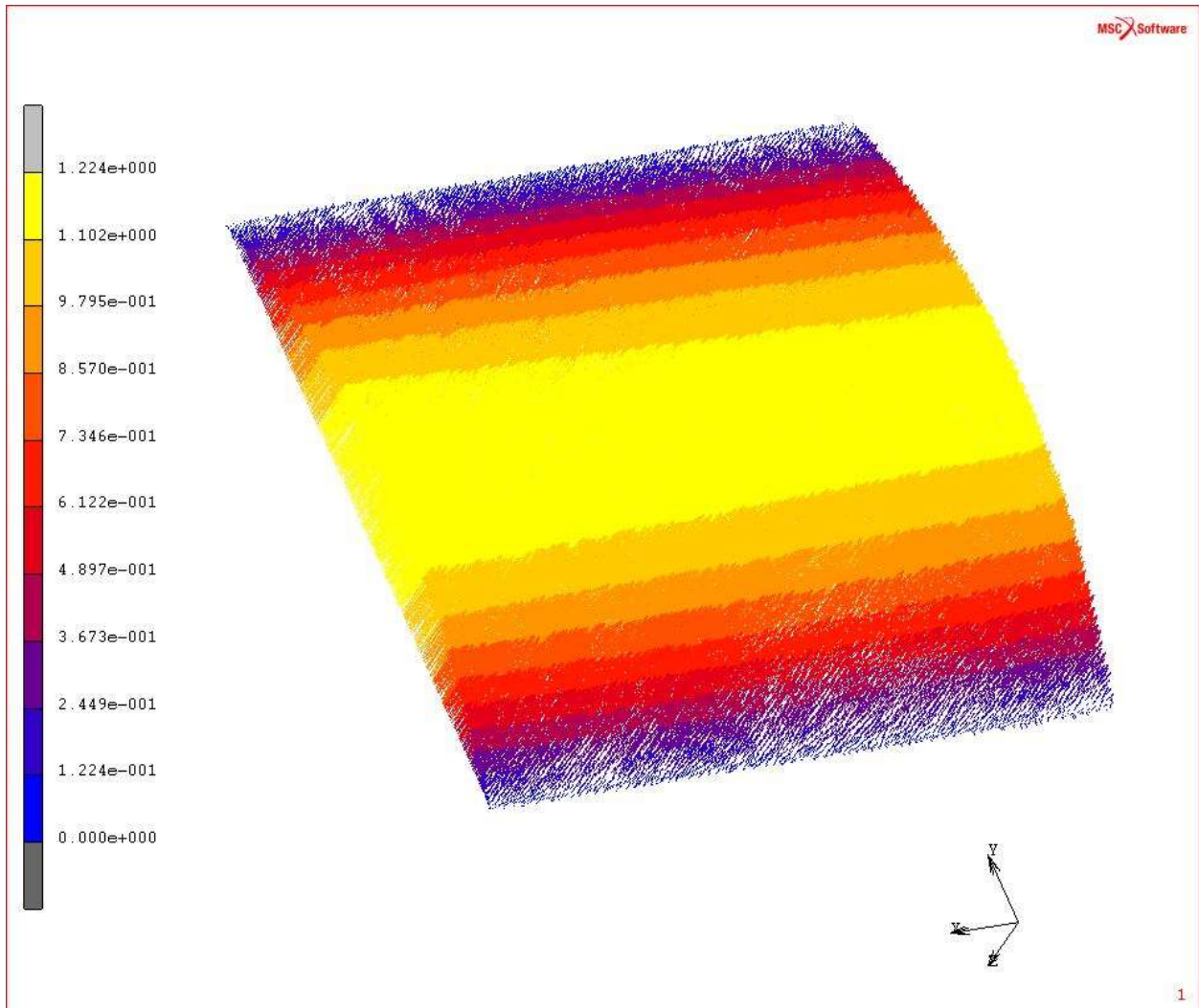


Figure 25 - Panel 3 vector plot after 15 second exposure at the 30 psi setting with a 1/2" Nozzle

The maximum displacement in panel 3 was nearly 1.22" after peening for 15 seconds. Again we see the maximum displacement remains consistent with the location seen in the pre-shot panel. The wider yellow band on the left of the panel indicates the largest displacement is on that side of the panel.

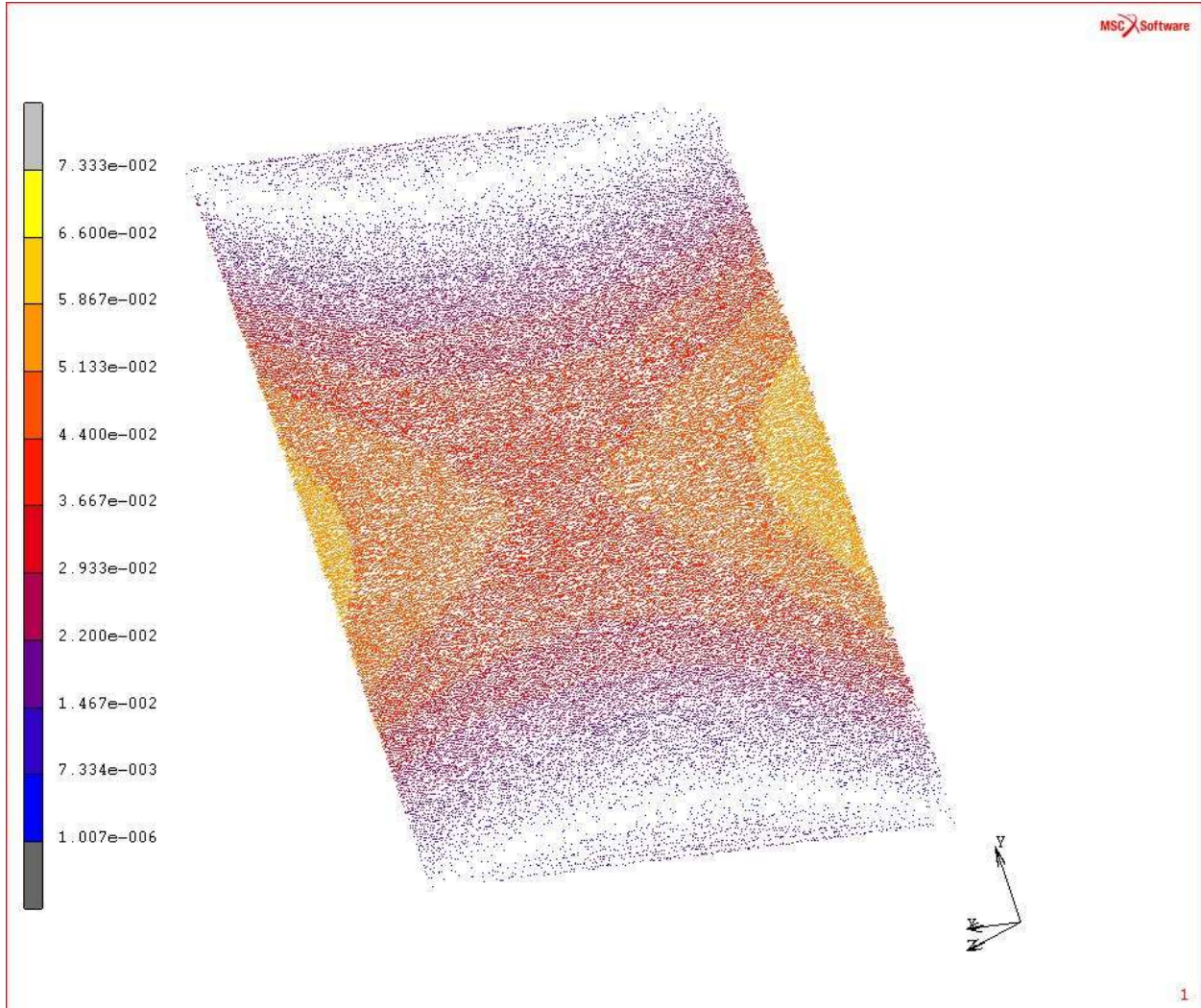


Figure 26 - Vector plot of panel 4 prior to shot peening

The pre-shot laser scan of Panel 4, shown in Figure 26, shows it's highest out of plane displacements near the middle of the right and left edges as shown. Again, the maximum pre-shot displacement is near 0.07 inch. This panel was then be exposed to a shot stream for 15 seconds/passes with a 1/2" nozzle and rescanned. The results are shown in Figure 27, where it can be seen the maximum out of plane displacement is increased to over 1.25 inch.

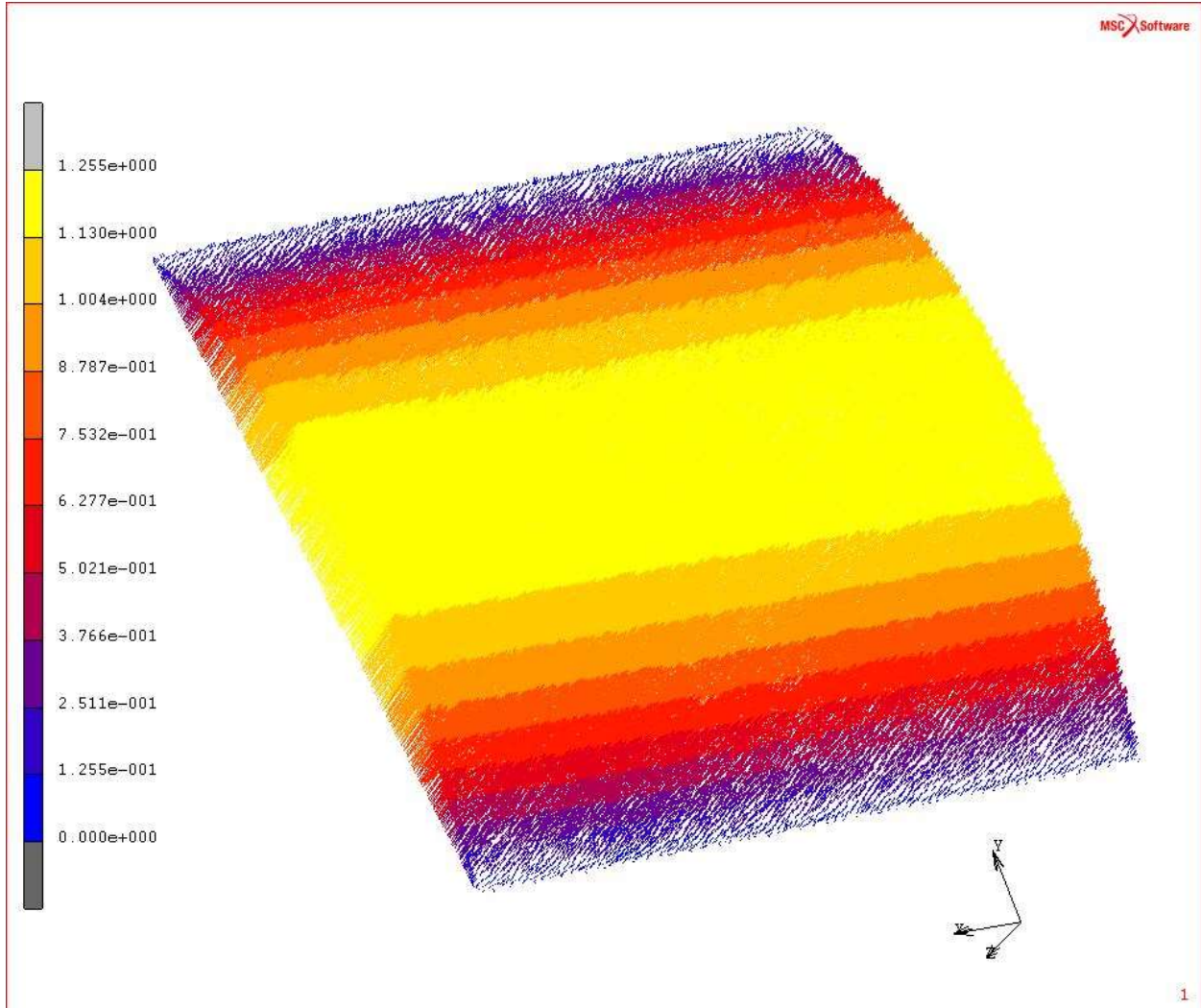


Figure 27 - Panel 4 vector plot after 15 second exposure at 30 psi setting with 1/2" Nozzle

Panel 4 does not seem to have retained the “hour glass” shape from left to right, that we saw before shot peening. The nearly straight regions of increasing displacement seem to indicate the center of the panel is very nearly the same as the edges. Although, since the displacement is so much greater after a 15 second/pass exposure, the slight “hour glass” shape seen before peening is simply not as noticeable.

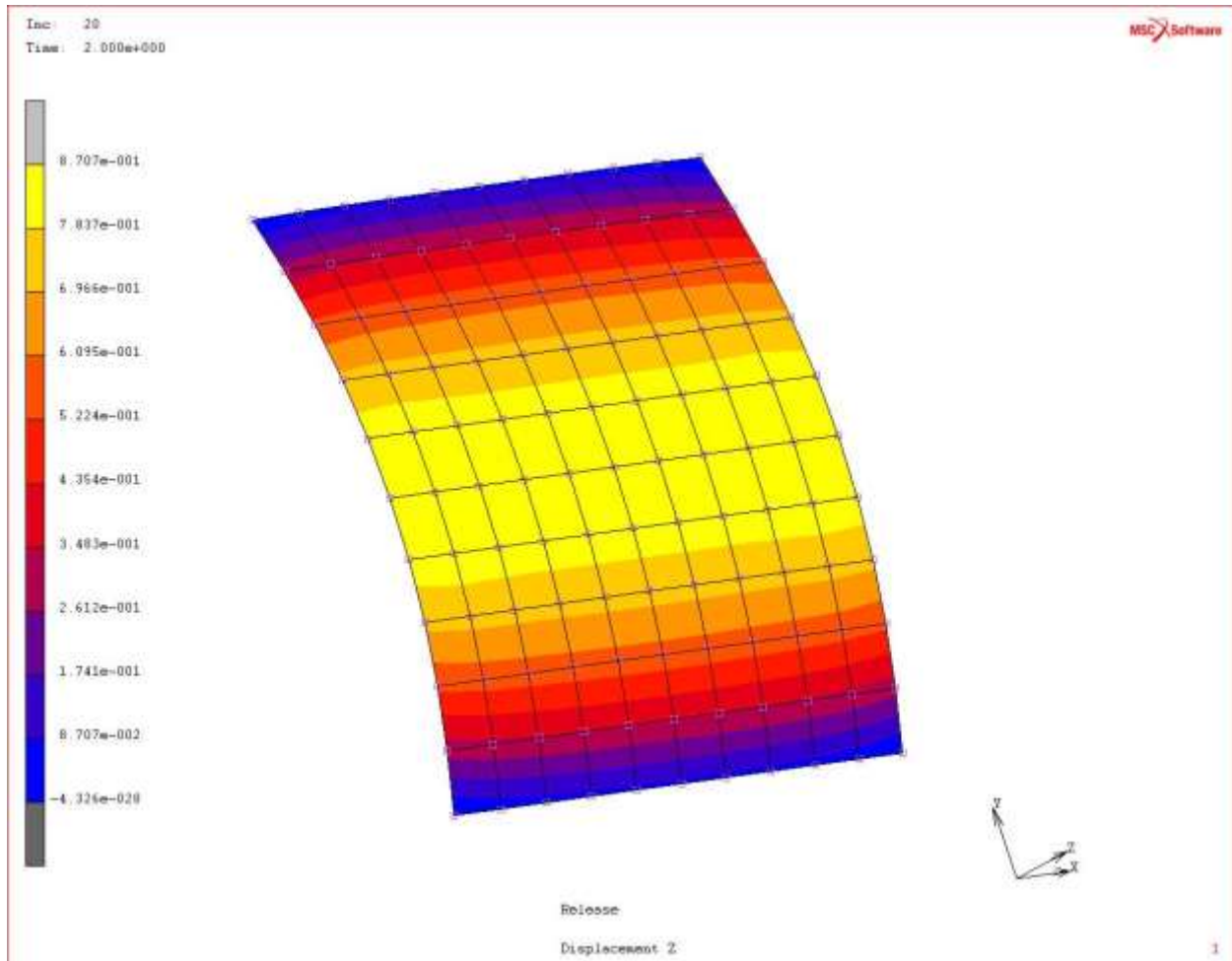


Figure 28 - FEA results using data from, 20 second exposure at 30 psi, residual stress measurements

Figure 28 shows the hybrid FEA result using data from a strip of the same aluminum material exposed for another 5 seconds. The difference in exposure produced out of plane results significantly lower than what was seen in the 10x10 panels exposed to a shot stream for 15 seconds/passes. Referring to Figure 16, you can see the lower arc height measured for a 20 second exposure as compared to a 15 second exposure. This “overpeened” state for the empirical data used in the FEA model resulted in difference noted. This error can be compensated for in future studies by interpolating the measurement data along the polynomial line shown for the aluminum strips, in Figure 16.

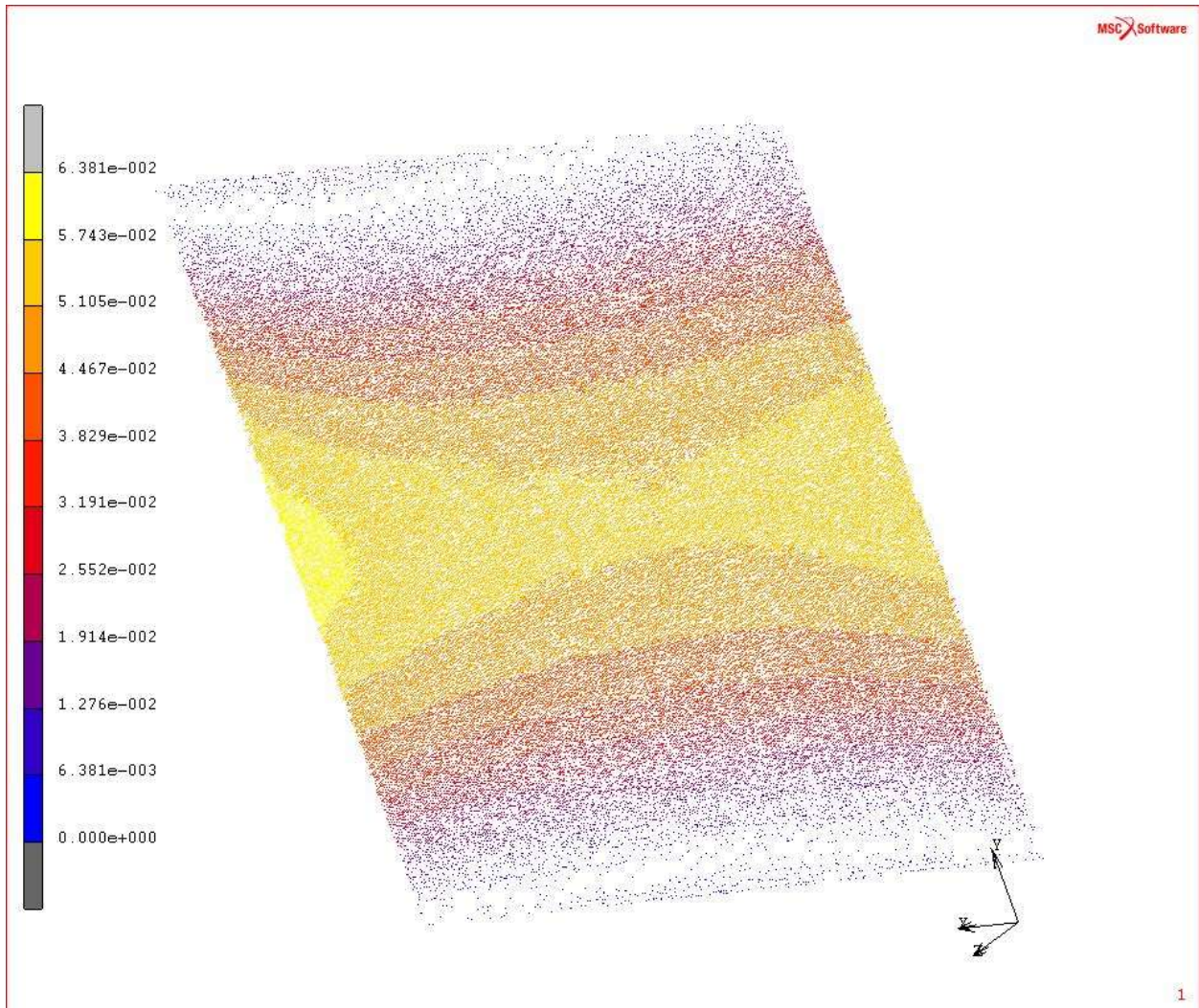


Figure 29 - Vector plot of panel 5 prior to shot peening

Panel 5's pre-shot laser scan, shown in Figure 29, displays the lowest initial out-of-plane displacement of the 10x10 inch panels used in this study. The initial displacement is only 0.064 inch. The hour glass shape seems to remain after shot peening, as can be seen in Figure 30. The maximum out of plane measurement after peening for 30 seconds with a 1/2" nozzle on a pressure setting of 30 psi is about 1.125 inch.

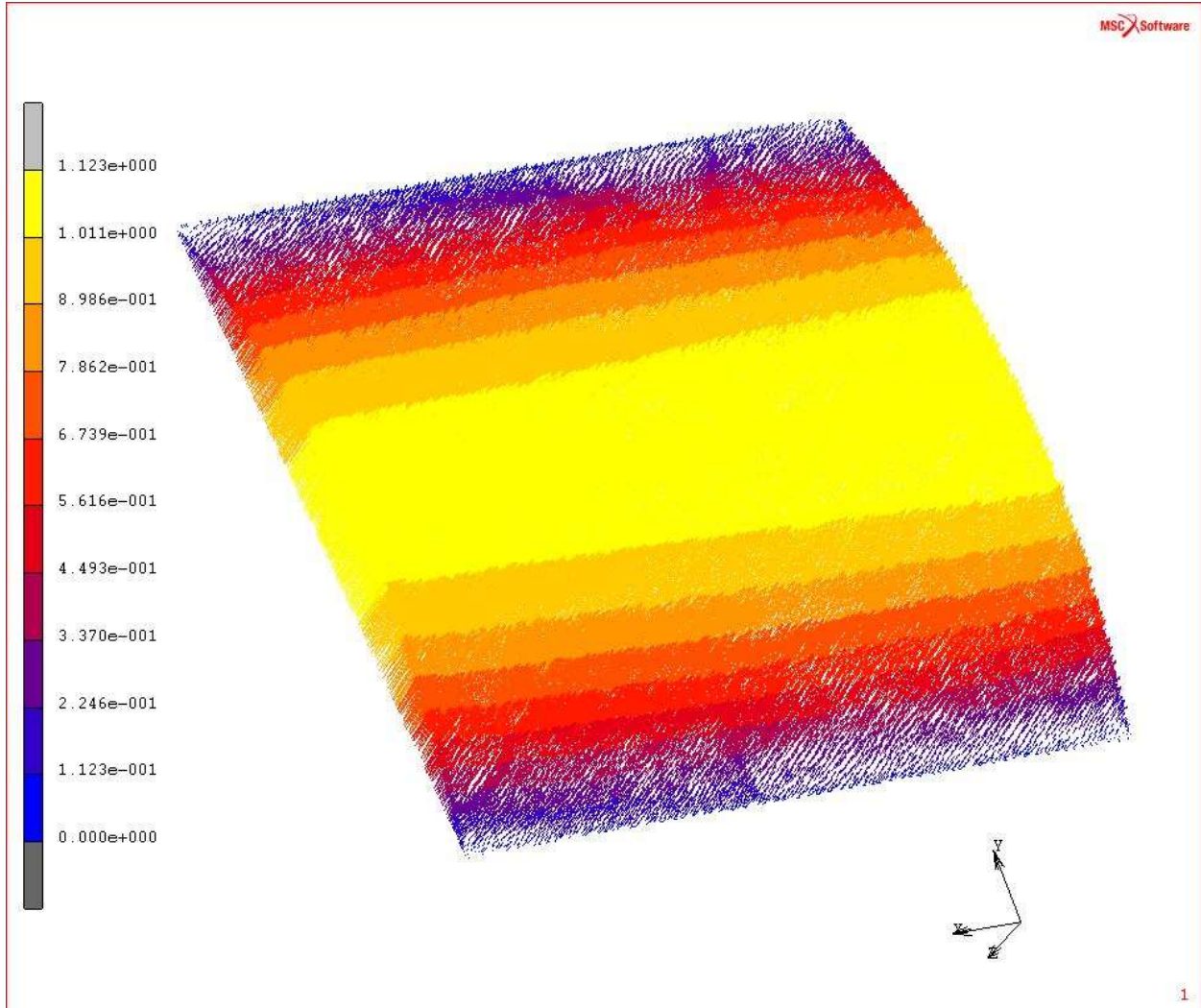


Figure 30 - Vector plot of laser scan of panel 5 following exposure to a 30 psi shot stream from a 1/2" nozzle for 30 seconds/passes

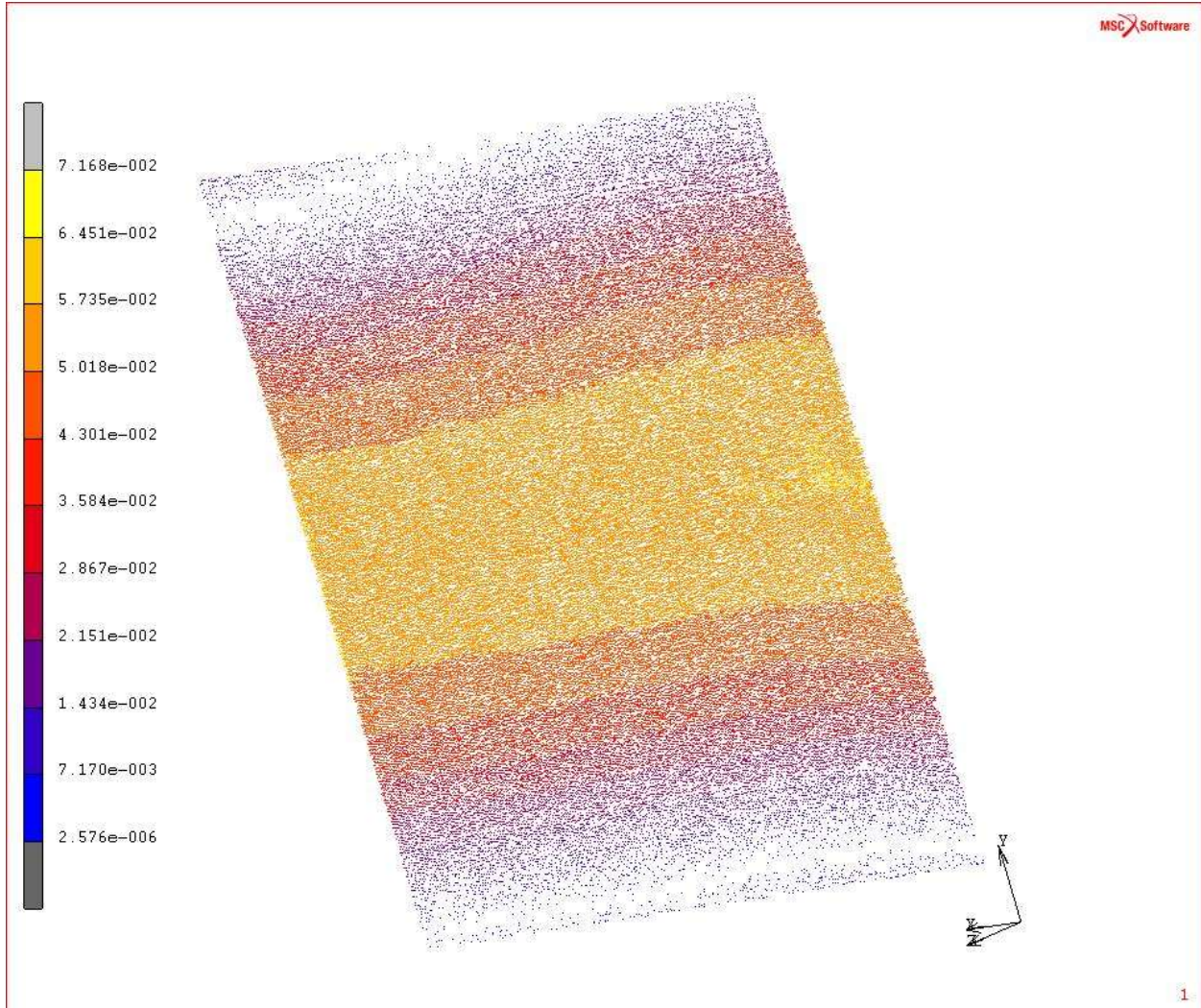


Figure 31 - Vector plot of laser scan of panel 6 prior to shot peening

Figure 31 shows the out plane displacement for panel 6 prior to shot peening. The maximum out of plane displacement in this panel is just over 0.070 inch. After shot peening this panel, like panel 5 also has a maximum out of plane displacement, measured by laser scanner, of nearly 1.125 inch. Figure 32 shows a wider yellow area on the left side of the figure, while Figure 31 shows the wider yellow band near the right of the figure. This is due to the parts being rotated 180° in orientation and is not due to the shot peen process. Future studies should also take care to keep the orientation consistent for clarity.

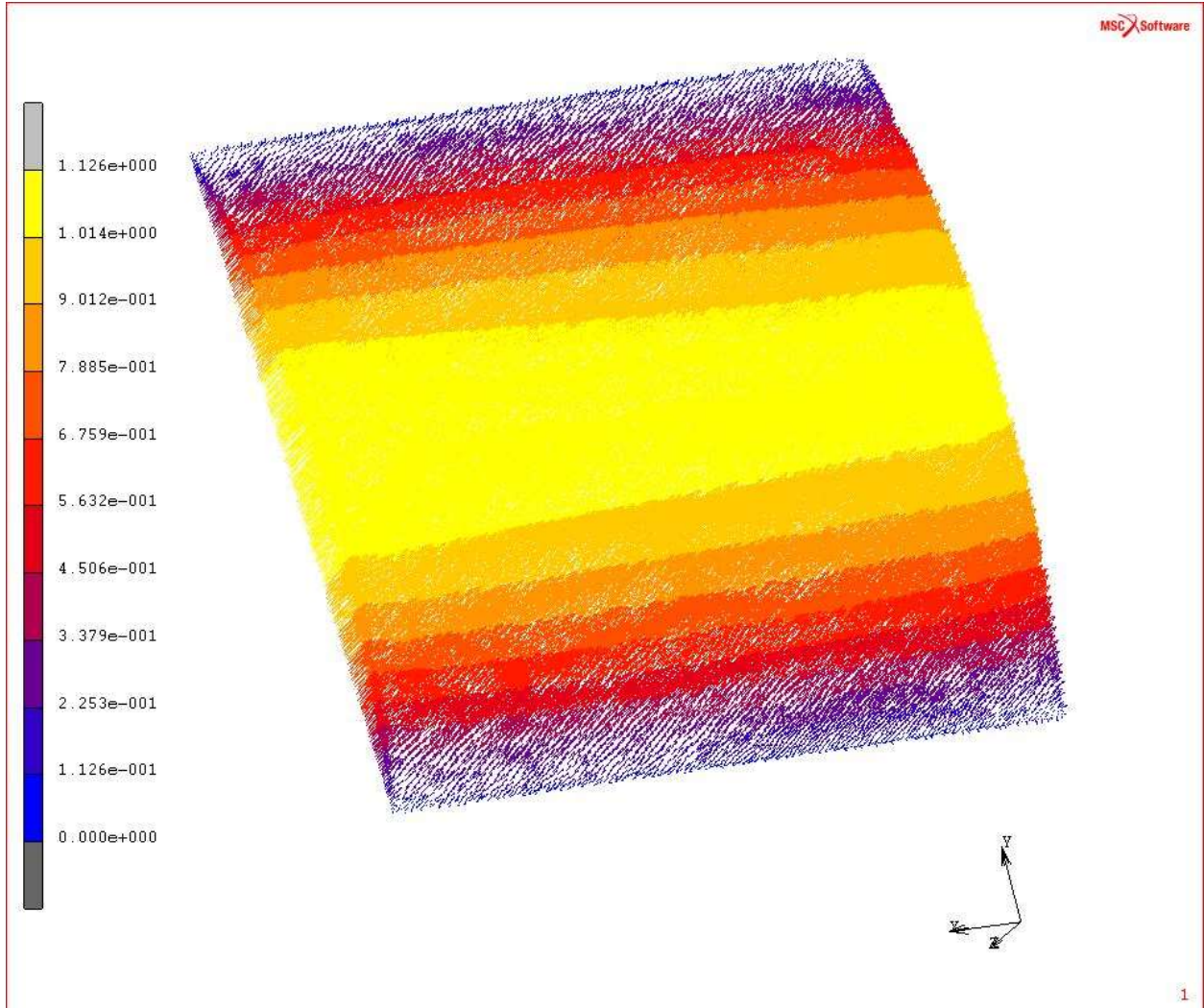


Figure 32 - Vector plot of laser scan of panel 6 after exposure to a 30 psi shot stream from a 1/2" nozzle for 30 seconds/passes

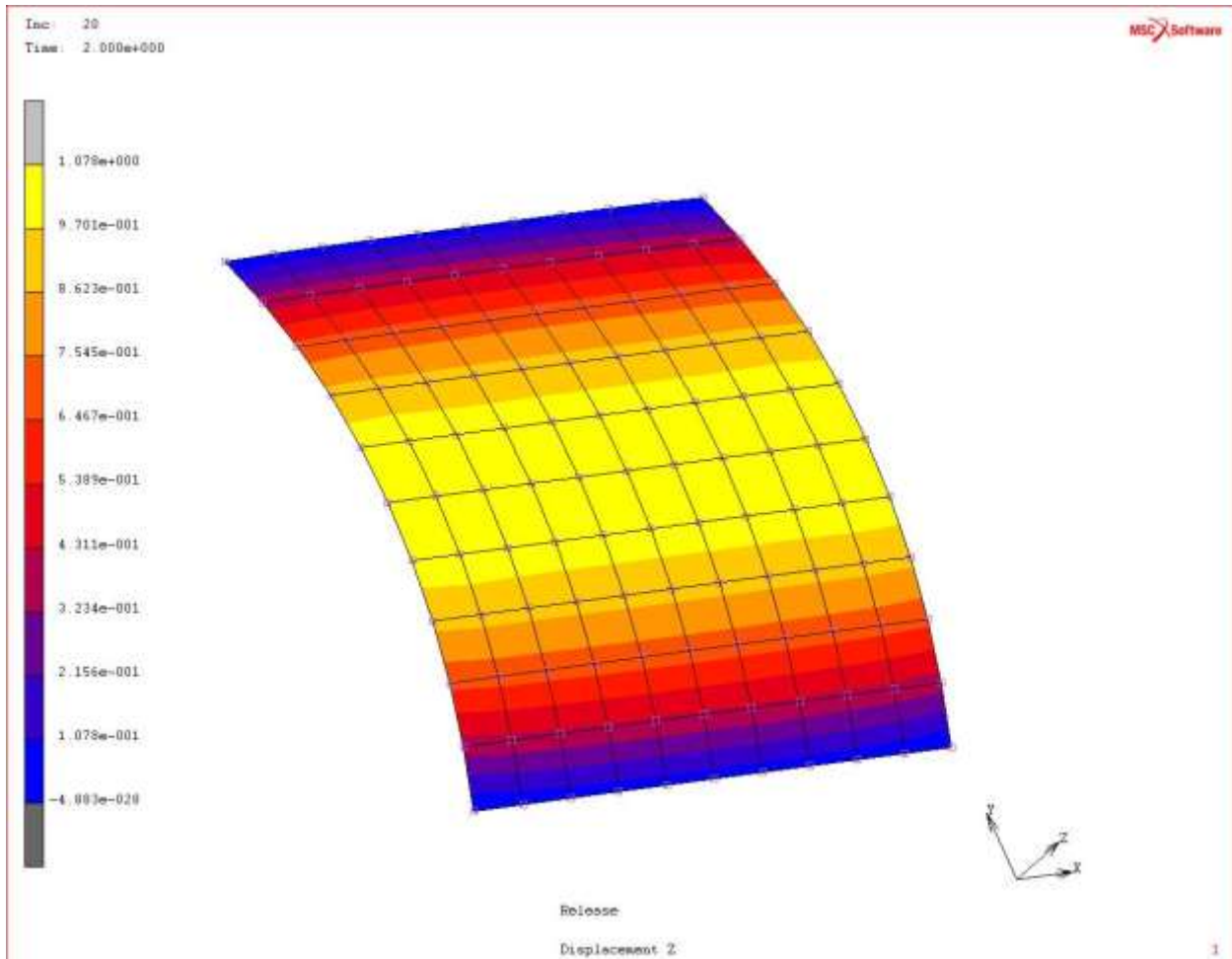


Figure 33 - Results of FEA shell model using residual stress data from an almen strip exposed to a 30 psi shot stream from a 3/8" nozzle for 35 seconds/passes

The hybrid FEA layered shell element model in Figure 33 used the empirical data from an aluminum strip made of the same aluminum, bare 7075-T6, as the six 10x10 panels. The data used in this model however was for a strip exposed for an additional 5 seconds than the panels in Figure 30 and Figure 32. As can be seen in Figure 16, the data levels off considerably after 15 seconds of exposure to the 30 psi stream. Although, two different nozzle sizes were used, the FEA model in this case produces a result within the initial displacement measured on the panels. Therefore, as noted before, more accurate results can be attained by incorporating initial out of plane displacements. Additionally accuracy can be attained by interpolation of the results or using directly correlated data sets.

3.2 Comparison of Empirical Data and Hybrid FEA Simulations

Table 1 shows a comparison of the deflection seen in the 10"x10" aluminum plates and the FEA model using residual stress measurements. It is seen that there is a close agreement between the predicted values from FEA and the experimental results.

Table 1 – Comparison of Shot Peened Panels and FEA model

Exposure	Empirical Arc Height (inches)	FEA	% Error
1 second, 30psi	0.5771, 0.6324	.5371	7%
15 seconds, 30 psi	1.224, 1.255	1.049	14%
30 seconds, 30 psi	1.123, 1.126	1.078	4%

The FEA model correlates rather well with the empirical data taken using the hole drill method. The initial deformation in all of the test panels, prior to peening, averaged around 0.070 inches. In the case of the 1 second and 30 second exposures, adding this existing deformation to the originally flat FEA model would bring the predictions even closer to the actuals.

There are however other reasons that may explain the differences in results. After reviewing the data, it was noted that even though the pressure setting were the same, the nozzle used to shot peen the almen strips was a 3/8 inch nozzle and the nozzle used to peen the test panels was a 1/2 inch nozzle. This surely will provide different line pressure and velocities of the shot.

Another factor was the restriction in resources needed to measure the residual stresses in the aluminum almen strips. Stress measurements were only taken for exposures of 1, 20 and 35 seconds/passes. As can be seen in Figure 12, the arc height measured at 20 seconds was lower

than that seen at 15 seconds. Since, the test panel exposure was 15 seconds this may well explain the large difference in results and could be avoided in production analysis using some type of interpolation or more accurate data.

The laser scanning method used to measure the test panels is very useful, but it is not beyond reproach. Care must be taken to make sure that the corners of the samples were touching the reference plane for proper comparison to the FEA results.

CHAPTER 4

4 CONCLUSIONS AND RECOMMENDATIONS

4.1 Conclusions

This thesis set out to propose a method for predicting deformations due to shot peen forming using FEA and residual stress measurements. The method proposed used the hole drill method to measure residual stresses in aluminum almen strips exposed to a shot stream for different periods of time and intensities, determined by pressure setting, of a manual shot peen process. The data collected was then applied to a layered 3D shell element model in a static finite element model to determine the deformation that was measured using a laser scanner on six 10 inch by 10 inch aluminum panels of the same thickness as the 0.050 inch thick aluminum almen strips.

The methods described in this paper have proven valid for pre-determining the deformation that will result from shot peening. More data needs to be collected to refine the models used in this thesis. Future work should be done to characterize different sizes and types of shot and substrates. Wire and glass beads are being used to perform the same type of process and would require additional testing. Much thicker parts are in need of rework when found to be outside of tolerance. Larger shot and perhaps higher velocities would be able to correct these parts.

As with any manual process there is variation that cannot always be controlled. It would be possible to completely automate the peen forming process such that a printer type of mechanism could be used to contour entire wing skins. This would be capable of producing repeatable net shaped contours and inducing compressive stresses should increase the fatigue life of the wing skins. The use of FEA to determine residual stresses can be a huge time and money

saver. This could lead to the residual stress management of all parts on aircraft and lead to more efficient and less costly designs.

4.2 Recommendations for Future Studies

Correlate arc height in materials to a primary stress/strain. As shown in Figure 7, the maximum stress induced is expected to occur near a certain depth. It would be worthwhile to further simplify this model and use a peak stress at a certain depth to make the analysis much quicker and remain accurate for deformation prediction.

Quantify and correlate energy input, shot velocity and mass, to induced stress and arc height. This research could have benefitted greatly from the use of a velocity measuring device. Unfortunately, none was available. It would be most interesting to know how the stream of energy used to cold work the material translates into residual stresses. The energy calculated by taking the area under a stress strain curve could provide a basis for calculating the efficiency of a forming process.

Obviously, studying the effect on just shot size on how stresses are induced in a substrate would be interesting also. It has been noted that the small shot draws the substrate towards the shot peened side, making it convex, while larger shot can be used to produce a concave surface.

The angle of incidence of the shot with the substrate should also be researched. This type of study could evaluate the energy transferred to indent formation and how substrate displacement is influenced. Friction would be an important aspect in such a study.

Nozzle size, for compressed air shot peening systems, could be evaluated to determine the effects on shot velocity and therefore intensity. I would expect the larger the nozzle size the lower the intensity from a shot stream if everything else remains constant.

More attention could be given to the amount of spring-back seen from different clamping/fixtures of the shot peened parts as well. The influence of how the part is held while being shot peened to the final shape would be an important aspect of predicting final shapes.

Finally, more efficient dynamic models may make it easier to study the effects of shot peening. Smooth Particle Hydrodynamic modeling of the shot stream or Arbitrary Lagrangian Eulerian methods may make the study of shot peening much easier in the near future.

REFERENCES

REFERENCES

1. (2008). *ASTM E837 - Standard Test Method for Determining Residual Stresses by the Hole-Drilling Strain-Gage Method*. ASTM.
2. (2008). *SAE J442 - Test Strip, Holder, and Gage for Shot Peening*. SAE International.
3. (2009). *SAE J2277 - Shot Peening Coverage Determination*. SAE International.
4. (2010). *SAE J443 - Procedures for Using Standard Shot Peening Almen Strip*. SAE International.
5. ASM International Handbook Committee. (1994). *ASM Handbook* (Vols. 05 - Surface Engineering). (J. S. C.M. Cotell, Ed.) ASM International.
6. Cao, W. F. (1995). Correlation of Almen arc height with residual stresses in shot peening process. *Materials Science and Technology Vol. 11 #9*, 967-973.
7. Champaigne, J. (2001). *Shot Peening an Overview*. www.shotpeener.com.
8. Gariépy, A., Larose, S., Perron, C., & Levesque, M. (2011). Shot peening and peen forming finite element modelling – Towards a quantitative method. *International Journal of Solids and Structures, Vol. 48*, 2859-2877.
9. Grasty, L. A. (1996). Shot peen forming sheet metal: finite element prediction of deformed shape. *Journal of Engineering Manufacture, Vol. 210*, 361-366.
10. Guagliano, M. (2001). Relating Almen intensity to residual stresses induced by shot peening: a numerical approach. *Journal of Materials Processing Technology*, 277-286.
11. Han, K. O. (2002). Combined finite/discrete element and explicit/implicit simulations of peen forming process. *Engineering with Computers*, 92-118.
12. Hollyoak, R., & Kirk, D. D. (2005). Relationship between Coverage and Surface Residual Stress. *Proceedings of the 9th International Conference on Shot Peening*, 373-378.
13. Kang, X. W. (2010). Multiple impact modelling for shot peening and peen forming. *Journal of Engineering Manufacture*, 689-697.
14. Kim, T. L. (2010). An area-average approach to peening residual stress under multi-impacts using a three-dimensional symmetry-cell finite element model with plastic shots. *Materials and Design*, 50-59.
15. Kirk, D. D. (2004). Prediction and Control of Indent Diameter. *The Shot Peener*, 18-21.

16. Kirk, D. D. (Fall 2009). Strip Factors Influencing Almen Arc Height. *The Shot Peener*, 26-32.
17. Kirk, D. D. (Spring 2009). Shot Peening Coverage: Prediction and Control. *The Shot Peener*, 24-32.
18. Kirk, D. D. (Summer 2010). Peening Indent Dimensions. *The Shot Peener*, 24-32.
19. Klemenz, M. S. (2009). Application of the FEM for the prediction of the surface layer characteristics after shot peening. *Journal of Materials Processing Technology*, 4093-4102.
20. Levers, A. P. (1998). Finite element analysis of shot peening. *Journal of Materials Processing Technology*, Vol. 80-81, 304-308.
21. MatWeb. (2013, April 20). *MatWeb*, (Cited May 2013). Retrieved from Material Property Data:
<http://www.matweb.com/search/DataSheet.aspx?MatGUID=9506f59dc73d41a7ab0da119f6775358&ckck=1>
22. Meguid, S. S. (1999). Three-dimensional dynamic finite element analysis of shot-peening induced residual stresses. *Finite Elements in Analysis and Design*, 119-134.
23. Meguid, S. S. (2002). 3D FE analysis of peening of strain-rate sensitive materials using multiple impingement model. *Journal of Material Processing Technology*, 119-134.
24. Miao, H. D. (2010). Experimental study of shot peening and stress peen forming. *Journal of Materials Processing Technology*, 2089-2102.
25. Miao, H. L. (2009). On the potential applications of a 3D random finite element model for the simulation of shot peening. *Advances in Engineering Software*, 1023-1038.
26. Schwarzer, J. S. (2002). Finite element simulation of shot peening - a method to evaluate the influence of peening parameters on surface characteristics. *Proceedings of the 8th conference of shot peening ICSP8* (pp. 507-515). Garmisch-Partenkirchen, Germany: Weinheim : Wiley-VCH, 2003.
27. Shivaswami, S., & Lankarani, D. H. (1997, September). Impact Analysis of Plates using Quasi-Static Approach. *Journal of Mechanical Design*, 119, 376-381.
28. Vishay. (2010). *Measurement of Residual Stresses by the Hole Drilling Strain Gage Method*. Vishay Precision Group.

29. Wang, T. P. (2002). Finite element impact modelling for shot peen forming. *Proceedings of the 8th conference on shot peening (ICSP8)* (pp. 540-546). Garmisch-Partenkirchen: Weinheim : Wiley-VCH, 2003.
30. Wang, T. P. (2006). A process model for shot peen forming. *Journal of Materials Processing Technology*, 159-162.
31. Zimmerman, M. S. (2010). Finite element modelling of coverage effects during shot peening of IN718. *International Journal of Materials Research*, 951-962.